THE JOURNAL OF BIOLOGICAL CHEMISTRY VOL. 290, NO. 9, pp. 5810–5825, February 27, 2015
© 2015 by The American Society for Biochemistry and Molecular Biology, Inc. Published in the U.S.A.

Differential Effect of Plant Lipids on Membrane Organization

*SPECIFICITIES OF PHYTOSPHINGOLIPIDS AND PHYTOSTEROLS**

Received for publication, July 28, 2014, and in revised form, January 8, 2015 Published, JBC Papers in Press, January 9, 2015, DOI 10.1074/jbc.M114.598805

Kevin Grosjean[‡], Sébastien Mongrand[§¶], Laurent Beney[‖], Françoise Simon-Plas[**], and Patricia Gerbeau-Pissot[‡1]

*From [‡]UMR1347 Agroécologie, ERL 6300 CNRS, Université de Bourgogne, 17 Rue Sully, BP 86510, 21065 Dijon Cedex, France, the [§]Laboratoire de Biogenèse Membranaire (LBM), CNRS, UMR 5200, F-33000 Villenave d'Ornon, France, the [¶]Laboratoire de Biogenèse Membranaire (LBM), Université de Bordeaux, UMR 5200, F-33000 Villenave d'Ornon, France, the [‖]Laboratoire Procédés Alimentaires et Microbiologiques, AgroSup Dijon, F-21000 Dijon, France, and **ERL 6300 CNRS, INRA, UMR1347 Agroécologie, 17 Rue Sully, BP 86510, 21065 Dijon Cedex, France*

Background: The effect of the wide variety of plant lipids on membrane organization is still poorly understood.
Results: The local amounts of phytosphingolipids and free and conjugated phytosterols control the relative proportion and spatial distribution of ordered domains.
Conclusion: Plant lipids differently modulate, alone or in combination, membrane heterogeneity.
Significance: Our results highlight how plant lipid diversity might drive the plasma membrane subcompartmentalization.

The high diversity of the plant lipid mixture raises the question of their respective involvement in the definition of membrane organization. This is particularly the case for plant plasma membrane, which is enriched in specific lipids, such as free and conjugated forms of phytosterols and typical phytosphingolipids, such as glycosylinositolphosphoceramides. This question was here addressed extensively by characterizing the order level of membrane from vesicles prepared using various plant lipid mixtures and labeled with an environment-sensitive probe. Fluorescence spectroscopy experiments showed that among major phytosterols, campesterol exhibits a stronger ability than β-sitosterol and stigmasterol to order model membranes. Multispectral confocal microscopy, allowing spatial analysis of membrane organization, demonstrated accordingly the strong ability of campesterol to promote ordered domain formation and to organize their spatial distribution at the membrane surface. Conjugated sterol forms, alone and in synergy with free sterols, exhibit a striking ability to order membrane. Plant sphingolipids, particularly glycosylinositolphosphoceramides, enhanced the sterol-induced ordering effect, emphasizing the formation and increasing the size of sterol-dependent ordered domains. Altogether, our results support a differential involvement of free and conjugated phytosterols in the formation of ordered domains and suggest that the diversity of plant lipids, allowing various local combinations of lipid species, could be a major contributor to membrane organization in particular through the formation of sphingolipid-sterol interacting domains.

Lateral partitioning of lipid domains was first reported in model systems, using biophysical approaches (1–4), indicating that the different lipid molecular species are not homogeneously distributed within lipid bilayers. Fluorescence microscopy studies using giant unilamellar vesicles (GUVs)[2] allowed observation of large domains of different composition, depending on the lipid mixture (5), suggesting that lipid heterogeneity may play a role in the spatial organization of biological membranes (6, 7). More recently, the lipid raft model proposed that the phase behavior of different lipid species could account for the lateral heterogeneity observed at the plasma membrane (PM) surface (8). Accordingly, optically resolvable imaging in lipid bilayer membranes involving at least three components reported the coexistence of a liquid-disordered (L_d) phase, formed mainly from unsaturated phospholipids (9–14), with a liquid-ordered (L_o) phase formed from saturated phospholipids and sphingolipids in the presence of cholesterol (8, 15, 16). In the latter, a higher degree of conformational order is imposed on the acyl tails of lipids by the rigid ring structure of cholesterol (17), increasing the thickness of the lipid bilayer and lipid packing, although lipids remain laterally mobile. Sterols (18) and sphingolipid/sterol interactions (19–24) have recently emerged as essential determinants of lipid partitioning within membranes.

Multiple roles for lipids in determining membrane order were thus emphasized and encompassed their tendency to phase separation and organization of biological membranes (25). However, all of these studies were performed on model and animal systems, where the lipid diversity is considerably lower than in plants. Plants contain a huge diversity of lipid molecular species, and the lipid mixture present in their PM is particularly complex. Lipidomic approaches revealed a PM

* This work was supported by the French Agence Nationale de la Recherche, program blanc, ANR "PANACEA" NT09_517917 (contracts to S. M. and F. S. P.) and platform Métabolome-Lipidome-Fluxome of Bordeaux (contribution toward lipid analysis equipment).
[1] To whom correspondence should be addressed. Tel.: 33-380693459; Fax: 33-380693753; E-mail: pgerbeau@dijon.inra.fr.

[2] The abbreviations used are: GUV, giant unilamellar vesicle; PM, plasma membrane; di-4-ANEPPDHQ, hydroxy-3-(*N*,*N*-dimethyl-*N*-hydroxyethyl)ammoniopropyl-4-(β-(2-(di-*n*-butylamino)-6-napthyl)vinyl) pyridinium dibromide; L_d, liquid-disordered; Lo, liquid-ordered; SG, steryl glycoside; GIPC, glycosylinositolphosphoceramide; GluCer, glycosylceramide; DOPC, 1,2-dioleoyl-*sn*-glycero-3-phosphocholine; DPPC, 1,2-dipalmitoyl-*sn*-glycero-3-phosphocholine; DiI-C_{18}, 1,1′-dioctadecyl-3,30,3′,3′-tetramethylindocarbocyanine perchlorate; laurdan, 6-dodecanoyl-2-dimethylaminonaphthalene; Bdp-cholesterol, 23-(dipyrrometheneboron difluoride)-24-norcholesterol; LUV, large unilamellar vesicle; RGP, red/green ratio of the pixel; RGM, red/green ratio of the membrane.

Downloaded from http://www.jbc.org/ at INRA Institut National de la Recherche Agronomique on April 21, 2015

composition of 30–50% phospholipids, 20–50% sterols, and 6–30% sphingolipids, depending on plant species and organs (for a review, see Ref. 26). The structural diversity found in plant lipids mainly arises from the biosynthesis of various combinations into each of these three lipid groups, which could reach to thousands of lipid species.

For instance, higher plant cells contain a vast array of sterols (61 sterols and pentacyclic triterpenes have been identified in maize seedlings) in which β-sitosterol, stigmasterol, and campesterol often predominate (27). Phytosterol molecular forms contain typically 28 or 29 carbons and, compared with cholesterol, exhibit an extra alkyl group, either an ethyl or methyl group, on the side chain in the C24 position and an extra carbon-carbon double bond in the sterol nucleus (28). In plant PM, steryl glycosides (SGs) and acyl steryl glycosides (ASGs) are found in addition to free sterols (29–33). Variations in sterol-conjugated forms originate from differences in the type of phytosterol; the sugar, usually the pyranose form of D-glucose; the configuration of the linkage; the number of sugar groups; and the sugar acylation. Acylation may occur at the C6 of the sugar moiety with fatty acids, palmitic acid (16:0) being most common (34, 35). SGs and ASGs, which do not exist in animal membrane, are more effective than free sterols at promoting hexagonal phase formation (36). They constitute up to ~30% of the detergent-resistant membrane fraction isolated from plant PM (26), based on their resistance to extraction by Triton X-100 at 4 °C (37).

Otherwise, sphingolipidomic approaches identified over 200 sphingolipids in *Arabidopsis* leaves (38). Glycosylinositolphosphoceramides (GIPCs), which may represent up to 60% of the plant PM, and glycosylceramide (GluCer) are the predominant sphingolipid classes (for a review, see Ref. 39). Although GIPCs belong to one of the earliest classes of plant sphingolipids to be identified (40–44), few GIPCs have been fully characterized to date because of their high polarity and relatively poor recovery using traditional extraction techniques (38, 45, 46). GIPCs are formed by the addition of an inositol phosphate to the ceramide followed by several glycosylation of the inositol headgroup (47–49). In the few plant species characterized to date, it seems that there is a dominant glycan structure with an hexose-glucuronic acid linked to the inositol, although the composition of the other sugars seems to be species-specific (50), polar heads containing up to seven sugars (for a review, see Ref. 51). GIPCs from *Arabidopsis* and tobacco, analyzed by mass spectrometry, were composed primarily of ceramide with t18:0 and t18:1 and 2-hydroxylated very long chain fatty acids (50, 51).

The role of such a wide diversity of plant lipids and the respective influence of the different classes of lipids on membrane organization are still poorly understood. To evaluate the specific involvement of each lipid molecular species in membrane organization, we added sequentially an equimolar amount of different lipids into phospholipid vesicles. To characterize the membrane lateral organization of such vesicles, we used hydroxy-3-(*N*,*N*-dimethyl-*N*-hydroxyethyl)ammoniopropyl-4-(β-(2-(di-*n*-butylamino)-6-napthyl)vinyl) pyridinium dibromide (di-4-ANEPPDHQ), an environment-sensitive fluorescent probe that was recently introduced as an alternative to 6-dodecanoyl-2-dimethylaminonaphthalene (laurdan) to assess the level of order of both model and biological membranes (52). Di-4-ANEPPDHQ is inserted into one leaflet of the lipid bilayer with its chromophore aligned to the surrounding tails of the lipid molecules and its headgroup oriented toward lipid polar heads. Its emission spectrum is thus influenced by the membrane packing around the dye molecules in the two lipid phases (53, 54) mainly by sensing the reorientation of solvent dipoles, related to the level of water penetration into the lipid bilayer (54). We thus described the individual ability of major phytosterols to modulate the global level of order of a phospholipid bilayer, in synergy with other sterol-conjugated forms and sphingolipids. We further analyzed, using multispectral confocal microscopy on large vesicles, the spatial distribution of the order level of membrane areas at a pixel (*i.e.* 300 × 300 nm) resolution. This revealed very different abilities of the various phytosterols, alone or in combination, to modulate the proportion of L_o phase and the membrane heterogeneity and a particular ability of GIPCs in synergy with conjugated sterols to organize the membrane and promote the formation of large ordered domains. We finally discuss how the diversity of plant lipids might drive the PM subcompartmentalization, allowing the dynamic segregation of membrane components.

MATERIALS AND METHODS

Commercial Reagents—1,2-Dioleoyl-*sn*-glycero-3-phosphocholine (DOPC), 1,2-dipalmitoyl-*sn*-glycero-3-phosphocholine (DPPC), cholesterol, and GluCer (corresponding to glucosylceramide purified from soybean and composed primarily (>98%) of ceramide with 4,8-sphingadiene (d18:2(Δ4,Δ8)) and α-hydroxypalmitic acid (h16:0)) were purchased from Avanti Polar Lipids, Inc. SGs (corresponding to a mixture of non-acylated steryl glycosides composed of ~56% β-sitosteryl glucoside, 25% β-campesteryl glucoside, 18% β-stigmasteryl glucoside, and 1% β-δ-5-avenosteryl glucoside), ASGs (corresponding to a mixture of acyl steryl glycosides mostly composed of β-sitosteryl glucoside palmitate), stigmasterol, and β-sitosterol were purchased from Matreya LLC. Campesterol was purchased from Sigma-Aldrich. All lipids were extemporaneously suspended in a chloroform/methanol (9:1, v/v) stock solution at 1 mg/ml.

Probes 1,1′-dioctadecyl-3,30,3′,3′-tetramethylindocarbocyanine perchlorate (DiI-C_{18}) and laurdan were purchased from Invitrogen; 23-(dipyrromethemeboron difluoride)-24-norcholesterol (Bdp-cholesterol) was from Avanti Polar Lipids, Inc.; and di-4-ANEPPDHQ was from Molecular Probes Inc. All stock solutions of dyes were stored in DMSO at −20 °C.

Extraction and Purification of Total GIPCs from BY-2 Cells—GIPCs are not commercially available; they were purified according to a method adapted from Carter and Koob (41) to obtain final amounts in the milligram range, described by Buré *et al.* (55). Briefly, tobacco BY-2 cells (~100–200 g, fresh weight) were blended with 400 ml of cold 0.1 N aqueous acetic acid in a chilled Waring Blendor at maximum speed for 2 min. The slurry was filtered under vacuum through 16 layers of acid-washed Miracloth on a large funnel. The residue was extracted twice again in the same manner. The aqueous acetic acid filtrate was discarded, and the residue was then re-extracted with hot (70 °C) 70% ethanol containing 0.1 N HCl. The slurry was fil-

Downloaded from http://www.jbc.org/ at INRA Institut National de la Recherche Agronomique on April 21, 2015

tered hot through Miracloth and washed with acidic 70% ethanol. The residue was re-extracted twice more with acidic 70% ethanol. The combined filtrates were chilled immediately and left at −20 °C overnight. The precipitate was pelleted by centrifugation at 2,000 × *g* at 4 °C for 15 min. The GIPC-containing pellet was washed with cold acetone until washes were colorless and finally with cold diethyl-ether to yield a whitish precipitate. GIPCs were then dissolved in tetrahydrofuran/methanol/water (4:4:1, v/v/v) containing 0.1% formic acid by heating at 60 °C, followed by gentle sonication. Glycerolipids were hydrolyzed by methylamine treatment, and GIPCs were re-extracted with hot 70% ethanol. GIPC extracts were further dried and submitted to a butan-1-ol/water (1:1, v/v) phase partition. This process left proteins and cell walls in the lower aqueous phase, whereas more than 97.5% of the GIPCs were recovered in the upper butanolic phase. Finally, the latter phase was dried, and the residue was dissolved in tetrahydrofuran/methanol/water (4:4:1, v/v/v) containing 0.1% formic acid. The amount of GIPCs was determined by quantitative GC-MS analysis measuring the 2-hydroxylated very long chain fatty acids, hallmarks of tobacco GIPCs.

Preparation of GUVs—GUVs were prepared by electroformation (56–58) to obtain unilamellar vesicles with sizes varying from 15 up to 50 μm. A flow chamber (ICP-25 perfusion imaging chamber, Dagan), connected to a function generator (PCGU1000, Velleman) and a temperature controller (TC-10, Dagan) was used for vesicle preparation. Briefly, various lipid solutions (4 μl of 1 mg/ml stock solution in chloroform/methanol (9:1, v/v)) were deposited on two microscope slides (18 × 18 mm) coated with electrically conductive indium tin oxide (resistivity 8–12 ohms). Lipid-coated slides were placed under vacuum for at least 2 h until a thin lipid film was obtained. Cover slides were set up on the flow chamber, and the lipid layer was rehydrated by 200 μl of 500 mM sucrose solution preheated to 55 °C. A voltage of 3.5 V at 10 Hz and a temperature of 55 °C were applied for a minimum of 2 h. After lipid swelling, the chamber was cooled down slowly to 22 °C (1 h minimum). The same procedure was used for all lipid mixtures.

Preparation of Large Unilamellar Vesicles (LUVs)—After being prepared as described above, GUVs were extruded and calibrated to 1-μm diameter on a hot plate (55 °C, corresponding to a temperature above the phase transition temperature of the lipid) by using a miniextruder from Avanti Polar Lipids, Inc. After 15 passes of the GUV solution through membrane, we obtained a homogenous LUV population (59, 60) with a diameter of 1 μm. LUVs were kept under a nitrogen atmosphere to minimize oxidation.

Fluorescence Spectroscopy—Probes (stock solution in DMSO) were diluted to 0.1 mol % in 500 mM sucrose solution. Fluorescence measurements were performed on a Fluorolog-3 FL3-211 spectrometer (Jobin-Yvon, Horiba Group) in the T-format with one double-monochromator for excitation and two single-monochromators for emission light. Detection is ensured by two photomultipliers. The light source is a xenon arc lamp. This spectrophotometer is equipped with movable excitation and emission polarizers. All fluorescence signals were recorded with emission and excitation bandwidths of 5 nm and systematically corrected from light scattering of an unlabeled sample. All data acquisitions were done with the Datamax software (Jobin-Yvon/Thermo Galactic Inc.). Experiments were done using a 10-mm special optic glass path cuvette filled with 1 ml of vesicle solution (4 μg/ml in 500 mM sucrose solution). All measurements were performed at 22 °C in a temperature-controlled chamber using a thermoelectric Peltier junction (Wavelength Electronics Inc.).

Confocal Fluorescence Microscopy—The vesicle suspension was labeled with fluorescent probes (di-4-ANEPPDHQ, DiI-C_{18}, or Bdp-cholesterol; stock solution in DMSO; 3 μM final) 5 min before microscopy observation and further placed between the slide and coverslip. All experiments were performed at room temperature (22 °C). A Sapphire LP (low power) continuous wave blue laser (Coherent) was used as the excitation source (488 nm). A Nikon C1Si/picoquant inverted microscope (Nikon) with spectral camera Nuance CRI was used to observe cells. Images were acquired with a plan apochromat ×100.0/1.40/0.13 oil objective. A dichroic slide (405–488 nm), which slightly modifies the emission spectrum in red wavelengths, was used to increase the fluorescent signal recovery. High spectral resolution was achieved through the use of a fine ruled diffraction grating, allowing a 5 nm channel resolution. The dispersed light was captured simultaneously at different wavelengths using 32 independent channels of a multianode array of photodetectors. Vesicles were observed by focusing on the maximum area of the vesicle membrane, and acquisition was performed for square surface (51.2-μm side lengths) at a 512 pixel resolution, according to the recommended sampling theorem (Nyquist) and resolution limit of the microscope.

Image Analysis—Individual recorded images were transferred to ImageJ software (National Institutes of Health). Red (or green) intensities were then computed by averaging four intensities from 545 to 565 nm (or from 635 to 655 nm). Ratiometric images were designed by dividing the created red images by created green images. To perform spatial analysis, pixels of 288 × 288 nm were analyzed, and central regions of the GUV top surface were cropped in order to avoid edge effects.

RESULTS

Major Phytosterols Differentially Modulate the Global Order Level of Model Membranes—The ability of each major phytosterol, individually or in combination, to modulate membrane order was investigated using the environment-sensitive probe di-4-ANEPPDHQ. Inserted in the whole bilayer, the dye locates with a slight preference into the L_d phase (54, 61), where its emission spectrum shows a red shift (62, 63). A function corresponding to the ratio of the fluorescence emission signal recorded at 550 and 660 nm, referred to hereafter as RGM (for red/green ratio of the membrane), gives a convenient and quantitative way to measure this emission shift (53, 54, 64–70). The RGM value allows characterization of the relative proportion of L_o and L_d phases in a lipid bilayer and is inversely correlated to the relative amount of L_o phase.

LUVs, homogeneously sized (1-μm diameter) to avoid any differential effect of the curvature on the fluorescence parameter recorded, were prepared using DOPC (33%), DPPC (33%), and sterol (33%): either cholesterol, stigmasterol, β-sitosterol, or campesterol. Lipid vesicles were labeled with di-4-ANEPPDHQ (3 μM), and the ability of each phytosterol to modulate

Downloaded from http://www.jbc.org/ at INRA Institut National de la Recherche Agronomique on April 21, 2015

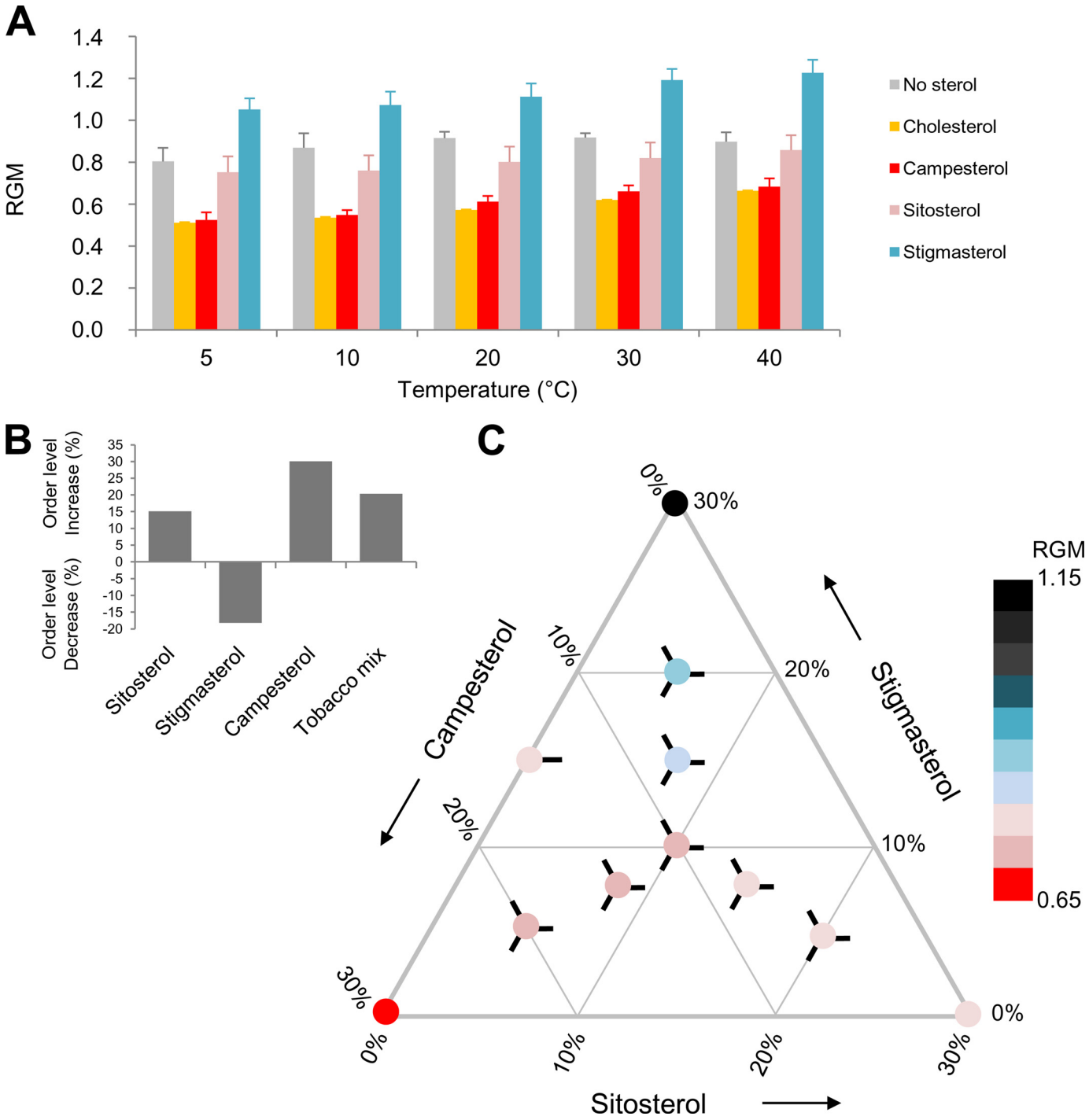


FIGURE 1. **The addition of free phytosterols differentially modulates the global order level of the membrane of DOPC/DPPC LUVs.** All data presented in this figure have been obtained by spectrofluorimetry after labeling of LUVs with di-4-ANEPPDHQ (3 μM). *A*, RGM of 1-μm diameter LUVs (DOPC/DPPC/phytosterol, 1:1:1 in molar weight) was measured for different sterols and at different temperatures ranging from 5 to 40 °C, as described under "Materials and Methods." Data shown are mean values ± S.D. (*error bars*) (n = 5 or more independent repetitions). *B*, illustrative effect of the ability of each phytosterol to increase or decrease membrane order was evaluated at room temperature. RGM measured for LUVs containing DOPC/DPPC/phytosterol (1:1:1 in molar weight) was normalized to the control value without sterol. The ratio was expressed as a percentage. *Tobacco mix*, a mixture of the major sterols found in the PM of 7-day-old tobacco suspension cells (34% stigmasterol, 33% campesterol, 32% sitosterol). *C*, illustrative phase diagram for a ternary lipid mixture containing DOPC/DPPC/phytosterol mixture (1:1:1 in molar weight). The phytosterol mixture corresponds to various amounts of campesterol, stigmasterol, and sitosterol. The RGM of LUVs was measured (at least 5 independent experiments), and the mean value was reported according to the *color scale*.

membrane order was evaluated through RGM quantification and assessed over a range of temperatures from 5 to 40 °C (Fig. 1*A*). The effect of each sterol on LUV membrane order level was only slightly enhanced by increasing temperature (Fig. 1*A*), and whatever the temperature, the same profile was observed (Fig. 1*A*). In detail, a strong ability of cholesterol to decrease the RGM value was observed, from 0.93 of LUV of DOPC/DPPC (1:1) to 0.56 upon cholesterol addition, at 20 °C (Fig. 1*A*), confirming that cholesterol efficiently increases membrane order level, as widely described in the literature (71–78).

Downloaded from http://www.jbc.org/ at INRA Institut National de la Recherche Agronomique on April 21, 2015

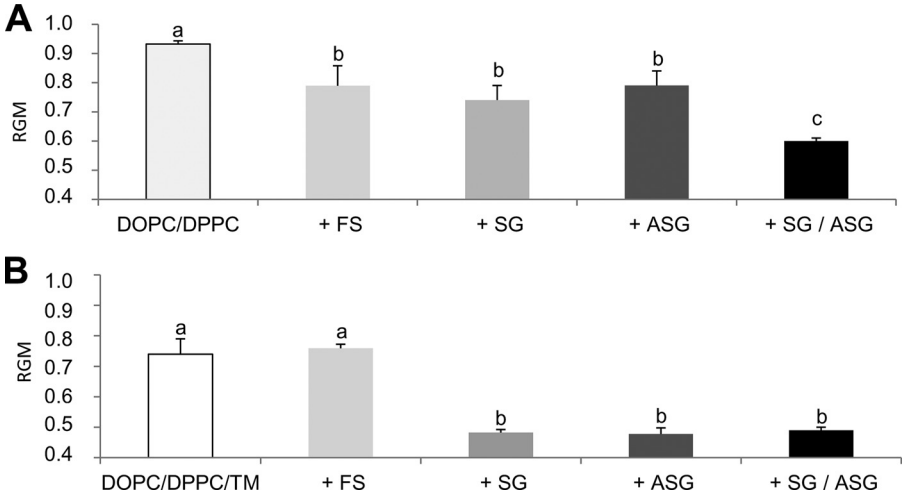


FIGURE 2. **Conjugated forms of phytosterols efficiently order membrane.** *A*, LUVs of 1-μm diameter were labeled with di-4ANEPPDHQ (3 μM). The RGM was measured by spectrofluorimetry, as described under "Materials and Methods," for different LUV mixtures, composed of DOPC/DPPC/sterol (1:1:1), sterol being either free (*FS*), sterylated (*SG*), or acylated (*ASG*) sitosterol or an equimolar combination of the latter two (*SG/ASG*). *B*, RGMs of LUVs composed of DOPC/DPPC/TM/conjugated or free sterol mixture (3:3:3:1) were characterized. *TM*, a lipid mixture of free sterols was added to mimic the sterol PM composition of tobacco suspension cells (34% stigmasterol, 33% campesterol, 32% sitosterol). Data shown are mean values ± S.D. (*error bars*) ($n < 9$ independent repetitions). The *different letters* indicate a significant difference ($p < 0.05$).

We checked that LUV production buffer did not change the RGM. When prepared on a pH-controlled buffer, such as PBS, we measured similar RGM (*e.g.* 0.58 ± 0.02 and 0.57 ± 0.02 for DOPC/DPPC/cholesterol (1:1:1) in sucrose buffer and PBS, respectively), showing that our results are applicable at physiological ionic strength.

Campesterol presented an effect close to the that of cholesterol, by decreasing the RGM to 0.65 at the same temperature (Fig. 1*A*). β-Sitosterol seemed less efficient at changing the membrane order level and decreased the RGM only to 0.79 (Fig. 1*A*). The same amount of stigmasterol induced a significant increase of RGM value up to 1.10, above the value recorded for LUV of DOPC/DPPC (Fig. 1*A*), suggesting its surprising potency to decrease membrane order level.

The sterol content of plant cell membranes is made up by a mixture of phytosterols, the properties of which had thus far not been investigated in combination. We therefore analyzed membranes of LUVs containing stigmasterol, β-sitosterol, and campesterol in different proportions, with a final concentration of total phytosterols of 33%. We first characterized the mixture corresponding to tobacco suspension cell PM (*i.e.* equimolar concentration (~10 mol %) of each phytosterol) (69). The RGM of such LUVs labeled with di-4-ANEPPDHQ significantly decreased from 0.93 to 0.74 ± 0.05 (S.D.), compared with control vesicles of DOPC/DPPC (1:1). Interestingly, this decrease of 20% reflects the sum of effects of individual phytosterol (Fig. 1*B*), suggesting that each sterol could participate, in an additive or subtractive way, in membrane organization. Fig. 1*C* shows the order level for LUVs of DOPC/DPPC/different mixtures of phytosterols (1:1:1). As campesterol concentration increases in the LUV mixture, RGM continuously decreases right up to its minimum value (0.65) reached at the maximum campesterol amount (33%, when campesterol is the only sterol used), suggesting that its ability to organize membrane depends on its relative concentration (Fig. 1*C*). The same is true for the two other phytosterols tested, stigmasterol and β-sitosterol; they modify the LUV order level, depending on both their own ability to modify membrane organization (Fig. 1*A*) and their relative concentration (Fig. 1*C*). Altogether, these results confirm the various abilities of different phytosterols to order lipid bilayers and reveal the individual and independent involvement of the different molecular species of phytosterols in the global order level of model membranes.

Conjugated Sterols Strongly Order the Membrane of LUVs—PM contains SGs and ASGs, which are specific to the plant kingdom and some bacteria. They are 1.6–3.4-fold enriched in detergent-resistant membrane fractions, suggesting their possible involvement in the formation of membrane ordered domains. When 33% of SGs or ASGs, mostly composed of conjugated β-sitosterol, were added to LUVs of DOPC/DPPC (1:1), the order level increased significantly, as indicated by the decrease of RGM (to 0.79 and 0.74, respectively; Fig. 2*A*). The decrease is similar to the one observed with free β-sitosterol (0.79; Fig. 2*A*), suggesting the same ability for free or conjugated forms of sterol to promote order in the lipid bilayer. When SG and ASG were used together, in an equimolar combination, a significant cooperativity to decreasing RGM was observed (Fig. 2*A*). Because the total amount of conjugated sterols incorporated in LUVs was maintained at 33%, whatever the combination of SG and/or ASG, this result suggests a strong synergistic ordering effect of the two different sterol-conjugated forms in the bilayer.

To further study possible interactions between different forms of free or conjugated phytosterols, 10% of an equimolar combination of SG and/or ASG was added to LUVs composed of DOPC/DPPC/free phytosterols (1:1:1). This proportion of conjugated sterols corresponds to the one currently found in plant cell PM (32). Although the extra addition of 10% free β-sitosterol did not induce any modification of RGM of LUVs of DOPC/DPPC/free phytosterols (1:1:1; Fig. 2*B*), supplementation with 10% SG, mostly sterylated β-sitosterol, triggered a decrease of RGM to a very low value of 0.48 (Fig. 2*B*). The same

Downloaded from http://www.jbc.org/ at INRA Institut National de la Recherche Agronomique on April 21, 2015

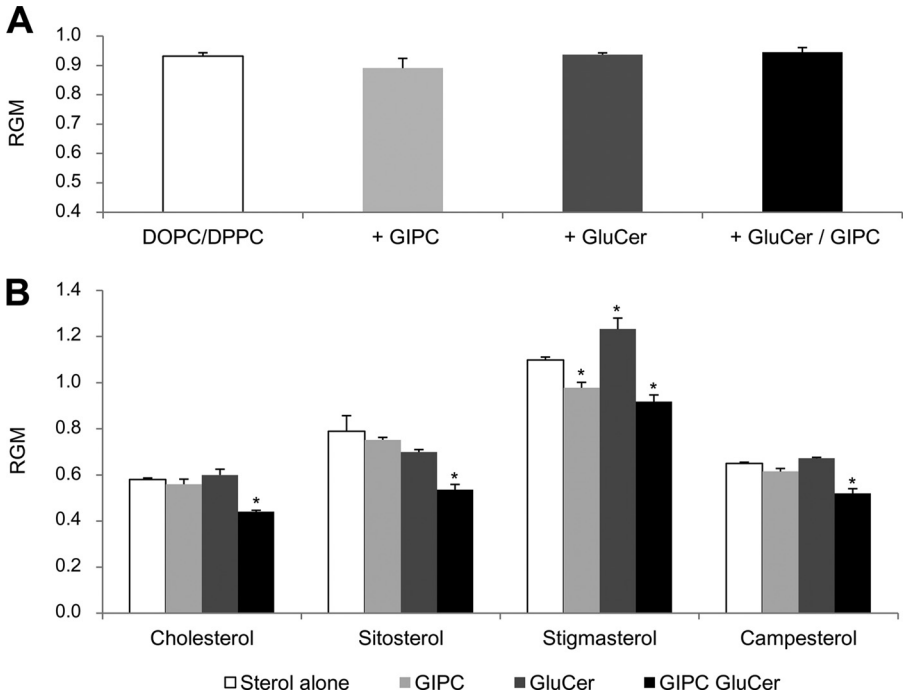


FIGURE 3. **Effect of sphingolipids alone and in combination with free sterols on membrane order level.** The RGM of 1-μm diameter LUVs of different compositions labeled with di-4ANEPPDHQ (3 μM) was measured by spectrofluorimetry in the absence (*white*) or presence of GIPC (*light gray*), GluCer (*dark gray*), or both GIPC and GluCer in equimolar combination (*black*). *A*, LUVs of DOPC/DPPC/sphingolipids (1:1:1). *B*, LUVs of DOPC/DPPC/sterol/sphingolipids (0.5:0.5:1:1); values of LUVs of DOPC/DPPC/sphingolipids (1:1:1) are shown in *white*. Data shown are mean values ± S.D. (*error bars*) ($n = 5$ or more independent repetitions). *, significant difference from control ($p < 0.05$).

effect was observed when ASG or SG/ASG together were added to LUVs containing free sterols (Fig. 2*B*). Altogether, these data indicate (i) that free phytosterols, SG and ASG, exhibit, alone, the same ability to increase membrane order; (ii) that a mixture of two different sterol forms is more efficient than free or conjugated sterols used separately; and (iii) that a combination of free and conjugated sterols is the most powerful way to increase membrane order.

Plant Sphingolipids Interact with Free Phytosterols to Increase the Order Level of Model Membranes—Although GIPCs are the predominant class of sphingolipids in plant cell PM (51, 79, 80), these molecular lipid species are not commercially available. We thus recently used a purification procedure described by Carter and Koob (41) modified by Bure *et al.* (55) on tobacco cell culture to obtain milligram amounts of GIPCs. The biochemical characterization and purity were controlled by GC-MS and TLC and revealed a 90% purified GIPC fraction, deficient in phytosterols and containing only 10% of glycerolipid contamination (phospho- and galactolipids). When 33% GIPCs were added to a DOPC/DPPC mixture (1:1), no significant change in the RGM of LUVs was observed (Fig. 3*A*). GluCer is also present in plant PM (38), free long chain bases and ceramides being far less abundant (13). When GluCer was added to LUVs of DOPC/DPPC (1:1), alone or with GIPC, the order level did not change significantly (Fig. 3*A*), suggesting no particular ability of plant sphingolipids, either separately or in combination, to modify the order level of model membranes containing only phospholipids.

When either GIPC or GluCer were incorporated into LUVs containing DOPC/DPPC/different phytosterols, to a final molar ratio of DOPC/DPPC/sterol/sphingolipids of 0.5:0.5:1:1, the order level did not change significantly (Fig. 3*B*), except with stigmasterol, for which a slight increase in the presence of GIPC and decrease with GluCer was observed (Fig. 3*B*). However, an equimolar mix of GluCer and GIPC (33% final sphingolipid concentration) significantly increased the order level of LUV membranes (Fig. 3*B*). The RGM decrease was observed whatever the phytosterol initially present in the vesicles, but it showed different intensities, with a reduction of 32, 20, and 16% for β-sitosterol, campesterol, and stigmasterol, respectively. These data suggest that the combinations of molecular species of sphingolipids and sterols present in plant PM may increase membrane order level and that such a synergistic effect depends on the molecular species of phytosterols.

Membranes of LUVs Containing a Complex Plant Lipid Mixture, Including Free Phytosterols, SG, and ASG, Exhibit Very High Order Level, with or without Phytosphingolipids—We finally used all of these different plant lipids together to evaluate the influence of the complexity of the lipid mixture on the membrane order level. As observed with pure sterol (Fig. 3*B*), no significant difference between RGM values of LUVs containing either DOPC/DPPC/free sterol tobacco mix (1:1:1), DOPC/DPPC/free sterol tobacco mix/GIPC (0.5:0.5:1:1), or DOPC/DPPC/free sterol tobacco mix/GluCer (0.5:0.5:1:1) was measured (Fig. 4*A*). However, the introduction of one conjugated sterol (SG or ASG, 10% final), together with a sphingolipid (GIPC or GluCer, 30% final), into LUVs induces a strong decrease of RGM (Fig. 4*A*), regardless of the molecular mixture of free phytosterol(s) (Fig. 4). A significant decrease (16–44%) of RGM up to very low values (between 0.35 and 0.61) is obtained, whatever the initial RGM value (Fig. 4*B*). These results, together with those presented in Figs. 2 and 3, support

Downloaded from http://www.jbc.org/ at INRA Institut National de la Recherche Agronomique on April 21, 2015

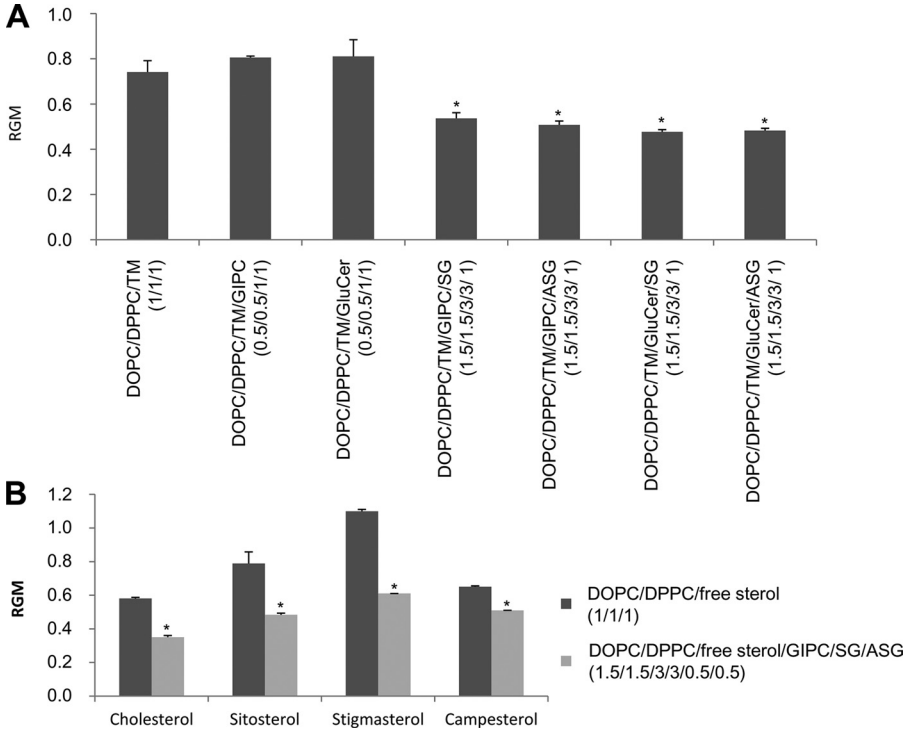


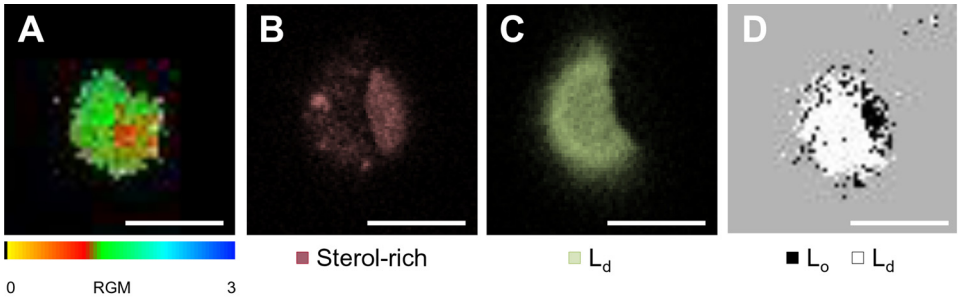
FIGURE 4. **A complex lipid mixture efficiently increases membrane order level.** The RGM of 1-μm diameter LUVs labeled with di-4-ANEPPDHQ (3 μM) was measured by spectrofluorimetry. GUVs were produced using different lipid mixtures; the proportion of each lipid is given in a molar ratio. *A*, LUVs composed of different lipid arrangements (*TM*, tobacco PM cell combination: 34% stigmasterol, 33% campesterol, 32% sitosterol) were compared according to their RGM values. *B*, LUVs composed of different lipid arrangements (where free sterol corresponds to either cholesterol, β-sitosterol, stigmasterol, or campesterol) were compared according to their RGM values. Data shown are mean values ± S.D. (*error bars*) ($n = 5$ or more independent repetitions). *, significant difference compared with the control corresponding to free sterols alone ($p < 0.05$).

the outstanding intrinsic ability of SG and ASG, separately or in combination, but independently of the presence of sphingolipid, to increase the order level of membranes.

Di-4-ANEPPDHQ Imaging Reveals Partitioning of L_o and L_d Domains at the Surface of GUVs—Spectrofluorimetry experiments described above were notably appropriate to measure the mean global order level of LUVs of many different compositions. To investigate the ability of different plant lipids to influence the spatial organization of the membrane, we next moved to confocal microscopy. GUVs with a diameter in the approximate range of 5–15 μm, suitable for optical microscopy, were prepared using electroformation with indium tin oxide-coated microscope slides. This methodology gives a high yield of GUVs, about 10^3 vesicles starting from 2 μg of lipids, most of them exhibiting a diameter greater than 10 μm. The emission signal of fluorescently labeled GUVs was acquired on a tangent plane corresponding to membrane surfaces of 100–350 μm^2 (*e.g.* see Fig. 5), allowing a spatial characterization of bilayer organization. The fluorescence intensity of di-4-ANEPPDHQ labeling was captured simultaneously at different wavelengths, and corresponding ratiometric images were designed measuring simultaneously the intensities between 545 and 565 nm and between 635 and 655 nm and then dividing the emission intensity of the two band pass filters by one another. A further pixel-to-pixel analysis of red/green ratio (RGP, for red/green ratio of the pixel) was performed to map the order level of the membrane (Fig. 5*A*), as achieved previously on the cell membrane (67). When used on a classical animal lipid mixture, DOPC/sphingomyelin (SM)/cholesterol (4.5:4.5:1), this method allows observation of the partitioning of reddish and greenish regions indicative of the coexistence of large L_o and L_d areas (Fig. 5*A*). Labeling of the same GUVs with laurdan, another widely used order-sensitive membrane dye, confirms such lateral organization of L_o and L_d phases (data not shown), according to results previously obtained (81).

We then examined on the same material the partitioning of the DiI-C_{18} (Fig. 5*B*) and Bdp-cholesterol (Fig. 5*C*), classical markers of the L_d (11) and sterol-enriched phases (82). Both fluorophores exhibited a spatial segregation in distinct domains (Fig. 5, *B* and *C*). Ratiometric images obtained with di-4-ANEPPDHQ were simplified to separate the RGPs corresponding to either L_o or L_d phases (Fig. 5*D*). To discriminate between L_o and L_d phase, we considered a threshold limit of 1.2 for RGP because pure DOPC GUVs exist in a unique L_d phase at room temperature (11, 81) and consistently exhibit more than 95% of their RGP values greater than 1.2. In these conditions, the pattern obtained with di-4-ANEPPDHQ (Fig. 5*D*) looks very similar to the ones obtained with classical fluorescent probes (Fig. 5, *B* and *C*), suggesting a striking correspondence between the L_o and the cholesterol-enriched phase on one hand and the L_d and DiI-C18 phases on the other hand. The proportions of L_o and L_d domains in different phase-separated GUVs deduced from RGP values are accordingly very similar to the one indicated by the partitioning of Bdp-cholesterol or DiI-C18 (Fig. 5*E*). A greater number of pixels with an RGP below 1.2 are counted when increasing cholesterol concentration, together with an increase of the area corresponding to Bdp-cholesterol accumulation (Fig. 5*E*), suggesting a close correspondence

Downloaded from http://www.jbc.org/ at INRA Institut National de la Recherche Agronomique on April 21, 2015



E

	Bdp-cholesterol fluorescence *(sterol-rich)*	Dil-C_{18} fluorescence *(L_d)*	RGM<1.2 *(L_o)*	RGM>1.2 *(L_d)*
DOPC/SM/Cholesterol (4.5/4.5/1)	16.9	70.4	28.0	72.0
DOPC/DPPC/Cholesterol (1/1/1)	54.5	48.3	51.4	48.6
DOPC/SM/Cholesterol (1/1/1)	48.1	43.3	47.1	52.9

FIGURE 5. **Spatial characterization of GUV membranes using a multiset of fluorescent probes.** GUVs corresponding to a mixture of DOPC/SM/cholesterol (4.5:4.5:1) were labeled with different fluorescent probes and observed in a tangent plane using confocal microscopy. *A*, di-4-ANEPPDHQ fluorescence emission signals were acquired in *red* and *green* band passes to design a ratiometric image as described under "Materials and Methods." The *red*/*green* ratios were measured for each pixel constituting the acquired surface area of labeled GUVs (RGP), and values were *pseudo-color-coded*. The *color scale* is reported, *hot colors* corresponding to a higher order level (low RGP). *B*, vesicles labeled with 3 μM Bdp-cholesterol, *red color* corresponding to those where the dye preferentially partitions (*i.e.* sterol-rich domains). *C*, vesicles labeled with 3 μM Dil-C_{18}; *green regions* were assigned to L_d domains, where the dye accumulates. *D*, to focus on the distribution of domains exhibiting the lowest order level, each pixel of a di-4-ANEPPDHQ fluorescent cell surface was classified according to its red/green ratio; the ones exhibiting a value below a fixed threshold of 1.2 are shown as *black pixels*. *A–D*, *bars*, 5 μm. *E*, the proportions of L_o and L_d phases, deduced from the spatial localization of the fluorescent probes in phase-separated GUVs described in *A–D* were compared. L_o and L_d enriched fractions were quantified and reported as percentages, depending on the fluorescent probe and the GUV lipid mixture.

between ordered domains (as revealed by di-4-ANEPPDHQ) and sterol-rich domains (as observed with Bdp-cholesterol).

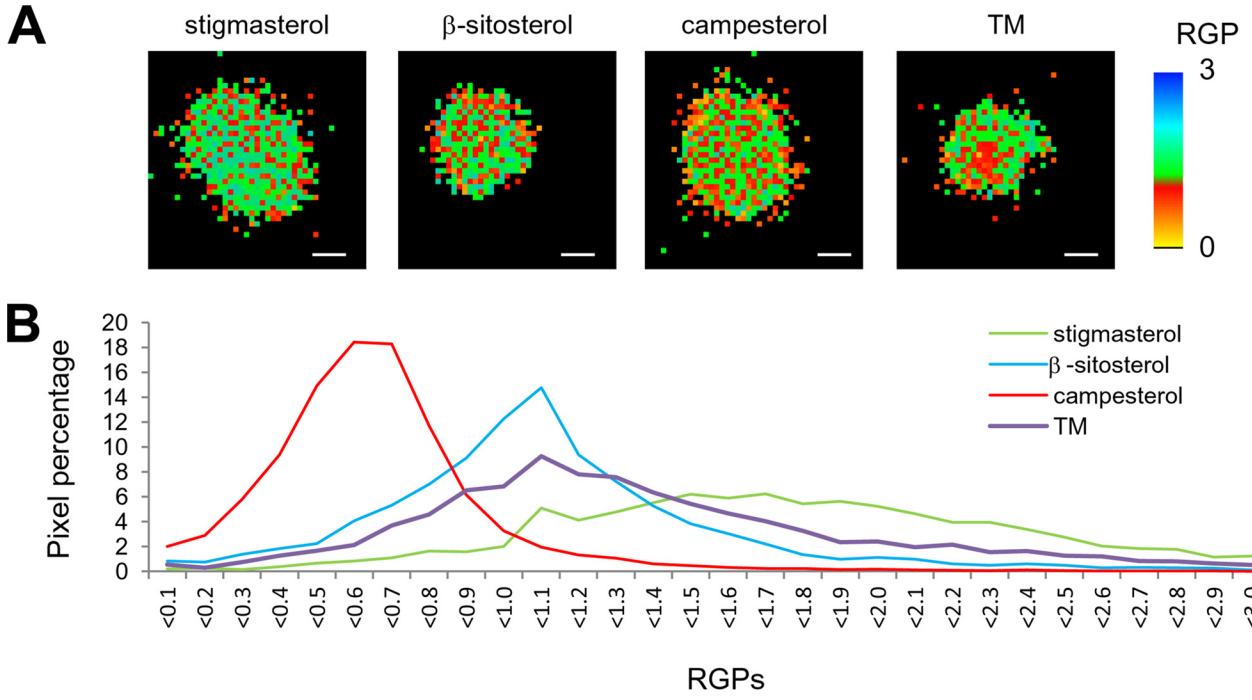
Free Phytosterols Exhibit Different Abilities to Spatially Organize Model Membranes and Create Ordered Domains—To investigate the spatial organization of membrane of GUVs composed of different mixtures of plant lipids, we analyzed the di-4-ANEPPDHQ emission spectrum of each pixel (288 × 288 nm) of the surface of these different vesicles (Fig. 6*A*), acquired as described above. Depending on the GUV composition, we clearly observed distinct organizations of reddish and greenish domains at the membrane surface (Fig. 6*A*) and, accordingly, different distributions of RGP values (Fig. 6*B*). For example, analysis of RGP values of DOPC/DPPC/stigmasterol vesicles revealed a continuous and flat distribution with a broad range of RGP values (from 0.5 to 3, in *green* in Fig. 6*B*). To precisely describe such RGP distribution, we measured its symmetry compared with a normal distribution using the Kurtosis value (Fig. 6*C*); data sets with Gaussian distribution exhibit a kurtosis of 0, and a negative kurtosis value reveals a uniform distribution that assigns equal probability to all RGP values. The flat shape exhibited by DOPC/DPPC/stigmasterol vesicles is thus in agreement with its negative kurtosis value (Fig. 6*C*), showing that no class of RGP value is significantly representative of the order level of these GUVs. This result suggests that, at this scale of observation, stigmasterol is not able to induce a spatial organization of the membrane into domains of a particular order level. On the contrary, GUVs containing β-sitosterol and campesterol exhibit a low RGM (Fig. 6*C*) and, accordingly, an RGP distribution centered on lower values, on 1.1 and 0.6, respectively (Fig. 6, *B* and *C*), consistent with their ability to order the membrane of LUVs (Fig. 1). RGP distributions were additionally sharper (Fig. 6*B*), in agreement with a positive Kurtosis value (1.8 and 2.4 for β-sitosterol and campesterol, respectively; Fig. 6*C*). Such peaked distributions indicate the predominance of few RGP values, corresponding here to domains with a high order level (visualized in *reddish colors* in Fig. 6*A*). Focusing on these L_o domains, we measured the representativeness of pixels of GUV membrane with an RGP of <1.2 (in *black* in Fig. 6*D*). The relative proportion of L_o phase among total pixels is strictly correlated to ability of each phytosterol to modulate the global order level of the membrane (*gray squares* in Fig. 6*E*). Furthermore, a granulometric analysis reveals a parallel between the ordering ability of a given phytosterol and its potency to promote large L_o domain formation (stigmasterol < β-sitosterol < campesterol; Fig. 6*F*). Altogether, our data propose various abilities of phytosterols to promote the formation and consequently the organization of L_o domains at the surface of model membranes.

Interestingly, the RGP distribution of vesicles containing a phytosterol mixture exhibits a flat distribution indicative of a high diversity of RGP values (Fig. 6*B*), confirmed by the negative Kurtosis value (Fig. 6*C*). The shape of this RGP distribution corresponds to the mean (both in the height and in the width) of the ones of each phytosterol constituting the mixture (Fig. 6*B*), in agreement with global RGM values (Figs. 2 and 6*C*). However, the L_o phase representativeness is much lower than the one predictable according to the corresponding RGM (Fig. 6*E*), and the few L_o domains found at the surface of GUVs constituted of tobacco mixture appear clustered (Fig. 6, *A* and *D*). GUVs constituted of DOPC/DPPC/phytosterol mixture exhibited thus a low L_o domain representativeness, similar to that of the stigmasterol (Fig. 6*E*), but the formation of domains bigger than 2 μm, as in campesterol (Fig. 6*F*). These results suggest a

Downloaded from http://www.jbc.org/ at INRA Institut National de la Recherche Agronomique on April 21, 2015

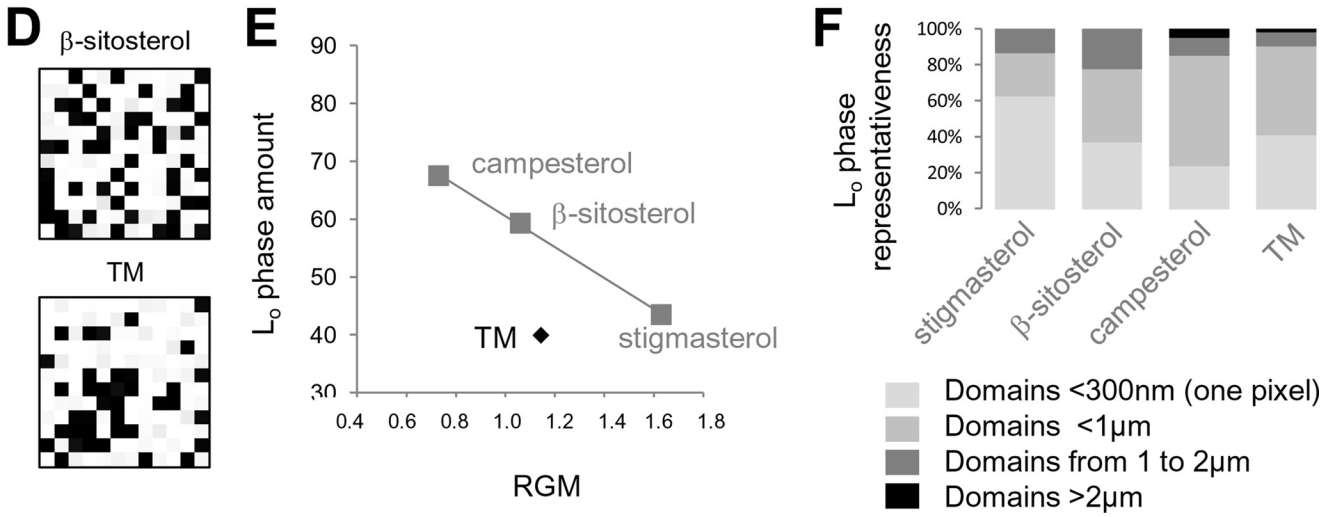
local cooperative effect of combined phytosterols to promote large L_o domain formation.

Involvement of SG and ASG, Saturated Fatty Acids, and GIPC in Spatial Organization of Model Membranes—DOPC/DPPC/sterol is a widely used mixture, well known to promote phase separation (14) and mimicking the saturated/unsaturated ratio found in plant cell. To evaluate the ability of plant sphingolipids to promote the formation of L_o domains that separate from unsaturated PC, we performed experiments using DOPC/phytosterol GUVs as target lipid vesicles (Fig. 7). GIPC supplementation to a final composition of DOPC/phytosterol/GIPC (1:1:1) slightly increases the membrane order level of such GUVs, as revealed by the RGM decrease observed, from 1.46 to 1.31 (Fig. 7*B*). Furthermore, the addition of GIPCs enables the

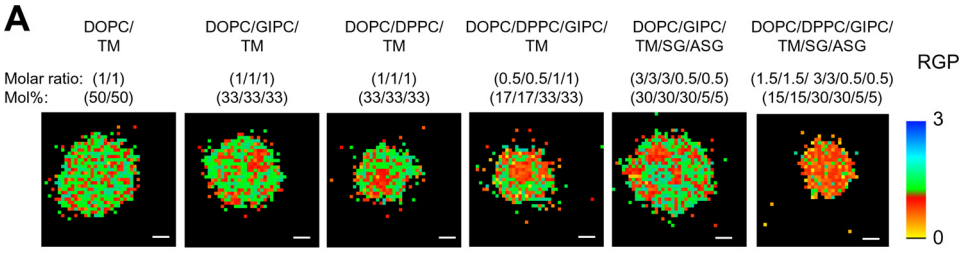


C

	stigmasterol	β-sitosterol	campesterol	TM
Kurtosis value	-1.5	1.8	2.4	-0.3
RGP value of the most abundant class	1.7	1.1	0.6	1.1
Amount of the most abundant class	6%	15%	18%	9%
RGM	1.63	1.06	0.73	1.14



Downloaded from http://www.jbc.org/ at INRA Institut National de la Recherche Agronomique on April 21, 2015



B

	DOPC/ TM	DOPC/GIPC/ TM	DOPC/DPPC/ TM	DOPC/DPPC/GIPC/ TM	DOPC/GIPC/ TM/SG/ASG	DOPC/DPPC/GIPC/ TM/SG/ASG
Order level	1.46	1.31	1.14	1.04	0.93	0.55
Ordered domains amount (%)	34	39	39	47	49	82
Large ordered domains (size>2μm, %)	0	1.3	1.4	4.9	7.5	14.3

FIGURE 7. **Plant lipids promote various spatial organization of membrane.** GUVs were produced using different lipid mixtures; the proportion of each lipid is given either in molar ratio or in mol % at the *top* of *A*. Tobacco mix (*TM*) represents a mixture of major sterols found in tobacco suspension cell PM (34% stigmasterol, 33% campesterol, 32% sitosterol). Vesicles used for *A* and *B* are identical. *A*, GUVs composed of different lipid mixtures were labeled with di-4-ANEPPDHQ (3 μM), and the fluorescence was recovered by multispectral confocal microscopy in a tangent plane, as described under "Materials and Methods." The RGPs were measured for each pixel (288 × 288 nm) constituting the membrane surface area of labeled GUVs and were *pseudo-color-coded* using the *color scale* reported at the *side*, *hot colors* corresponding to higher order level (low RGP). *B*, characterization of model membrane spatial organization. Global order level was measured as mean RGP value. Focusing on pixels exhibiting an RGP value below a fixed threshold of 1.2 (ordered domains), their amount was reported for the different GUV mixtures according to their relative abundance (expressed as the percentage of pixels exhibiting an RGP value below 1.2, relative to the total amount of pixels). The representativeness of large ordered domains (>2 μm) was expressed as the percentage of pixels present in such domains among all pixels exhibiting an RGP below 1.2.

detection of groups exhibiting a size over 2 μm (Fig. 7*A*) without modification of the relative amount of L_o phase (Fig. 7*B*). GIPC-induced L_o domain production exhibited an intensity similar to that induced by saturated fatty acid addition (Fig. 7*B*), even if the global order level was higher for DOPC/DPPC/phytosterol vesicles (1:1:1) than for DOPC/GIPC/phytosterol vesicles (1:1:1; Fig. 7*B*). Interestingly, an additive effect of sphingolipids and saturated fatty acid forms of PC was observed in DOPC/DPPC/GIPC/phytosterol mixture vesicles (0.5:0.5:1:1). Indeed, an enhancement of order level was measured, with an RGM decreasing to 1.04 and the relative amount of L_o phase rising to 47%, nearly 5% of which appeared as domains with a size over 2 μm (Fig. 7*B*).

Finally, the introduction of SG/ASG (5% final each) in vesicles of DOPC/GIPC/TM (30% final each) induced a shift to lower RGP values (Fig. 7*A*), consistent with the decrease of RGM (Fig. 7*B*), indicative of an increase of membrane order level, and with the increase of proportion of large ordered areas (Fig. 7*B*). When SG/ASG (5% final each) were incorporated into vesicles of DOPC/DPPC/GIPC/TM (15:15:30:30% final), the RGM decreased drastically, in agreement with a strong increase of low RGP values (Fig. 7*A*), the L_o phase representativeness rising up to 82% (Fig. 7*B*). Although tricky due to the very high proportion of ordered phase, a granulometric approach reveals the formation of very large L_o domains, with about 15% of L_o phase present within domains above 2 μM size. Altogether, our results propose the ability of GIPC and DPPC to increase membrane order level, similarly as observed previously with SM and DPPC (83), and also to promote L_o domain aggregation. Moreover, a synergy is observed when GUVs are supplemented with the two lipid species together, and the strongest enhancement is seen when saturated and unsaturated PC, free and conjugated sterols, and sphingolipids are all represented. The diversity of lipid species contained in GUVs surprisingly led to the formation of an L_o area that covered almost the entire membrane surface, suggesting that all lipids could be among the main actors involved in the membrane order level heterogeneity.

DISCUSSION

Free and Conjugated Phytosterols Exhibit Various Abilities That Could Act in Combination to Order Lipid Bilayer—The first investigations identified a planar ring system, a 3β-hydroxyl group, and an isooctyl side chain requirement for cholesterol's ability to organize membrane and the Δ^5 double bond involvement in cholesterol-phospholipid interaction (84). Major plant sterols all satisfy these conditions and are accordingly able to stabilize lipid bilayer (85), to order phospholipid acyl chain, and consequently to reduce membrane water per-

FIGURE 6. **Free sterols promote various spatial organization of membrane.** All experiments were performed using GUVs composed of DOPC/DPPC/phytosterol (1:1:1), sterol being either stigmasterol, β-sitosterol, campesterol, or tobacco mix (*TM*), which represents a mixture of major sterols found in tobacco suspension cell PM (34% stigmasterol, 33% campesterol, 32% sitosterol). For all lipid mixtures, the final concentration of total sterols was 33 mol %. *A*, GUVs composed of different lipid mixtures were labeled with di-4-ANEPPDHQ (3 μM), and the fluorescence was recovered by multispectral confocal microscopy in a tangent plane, as described under "Material and Methods." The RGPs were measured for each pixel (288 × 288 nm) constituting the membrane surface area of labeled GUVs and were *pseudo-color-coded* using the *color scale* shown at the *side*, *hot colors* corresponding to higher order level (low RGP). *B*, distribution of RGP values of individual pixels of the membrane of GUVs and influence of the different phytosterols. The *x* axis corresponds to the class of RGP values, and only the maximal value of each class is reported on the graph. The *y* axis corresponds to the percentage of each class. *C*, characterization of RGP distribution, reporting the peak and the Kurtosis value (for more details, see "Materials and Methods"). *D*, central regions (3.5 × 3.5 μm) of the GUV top surface were cropped in order to avoid edge effects, and pixels exhibiting a RGP value below a fixed threshold of 1.2 were *colored* in *black*. *E*, the density of *black pixels* was evaluated and correlated to the global RGM. *F*, the size of *black pixel* groups was evaluated for the different GUV mixtures and reported according to their relative abundance. Data shown are mean values (n = 21–37 GUVs).

Downloaded from http://www.jbc.org/ at INRA Institut National de la Recherche Agronomique on April 21, 2015

meability (86), although less efficiently than mammalian sterol (87–89). Here, we described a strong ordering ability for campesterol, in the same range as the cholesterol one, and a less efficient one for β-sitosterol (Fig. 1). Accordingly, campesterol exhibits a high potency to stabilize DPPC bilayer (90) and to tightly pack the phospholipid bilayer (91, 92), which has been attributed to its smaller freedom of rotation at the C17-hydrocarbon chain. Stigmasterol was previously found to have a much weaker ordering effect than other sterols on diphenylhexatriene anisotropy (93). In agreement, we described here its lack of ability to order lipid bilayer (Fig. 1) and accordingly to promote L_o phase formation (Fig. 6). Measurements of parinaric acid fluorescence polarization have similarly shown that stigmasterol is unable to obliterate phospholipid phase transition and to interact with L_o phase, whatever the phosphatidylcholine analog used to produce target lipid vesicles (94). Our data thus confirm the specific capacity of phytosterols to modulate the order level of phospholipid bilayers (stigmasterol < β-sitosterol < campesterol), by using RGM as a new parameter. Such individual phytosterol ability to order membrane was found to only slightly depend on temperature, as previously demonstrated for DOPC/DPPC/cholesterol vesicles (84). Indeed, below 40 °C, the temperature at which the L_o and L_d domains separated in the presence of 33% cholesterol (84), RGM measurement assesses the global order level without taking into account local and dynamic phase transitions.

However, phytosterols exist within plant PM as a mixture of stigmasterol, campesterol, and β-sitosterol, relative amounts of which vary among plants, tissues, and growth conditions. For example, the β-sitosterol/stigmasterol ratio in the membrane has been known to influence the response of a cell to various biotic (95) or abiotic stresses (*e.g.* in the resurrection plant *Ramonda serbica* following dehydration and rehydration (96) and in broccoli root in response to salt stress (97)). Using vesicles containing different phytosterol mixtures, we clearly showed that the relative amounts of each phytosterol finely control the membrane order level (Fig. 1), which may be meaningful to allow plant adaptive responses to changes in environmental conditions. In agreement, using sterol biosynthesis mutants, a higher level of stigmasterol within plant PM has been correlated with altered fluidity and permeability characteristics (*e.g.* a restricted solute efflux) (98, 99). Furthermore, the relative increase of more planar sterols, such as campesterol, reduced the membrane permeability to charged ions (87, 100) and might favor ion exclusion. The molar ratio between more and less planar sterols thus plays a fundamental role in allowing the plant to tolerate abiotic stress because the ratio is considered to be an index of membrane permeability and functioning (101). Although the precise mechanism by which phytosterols, in combination, regulate membrane properties is not yet understood, we show here that their diversity is a powerful tool, through the relative amounts of their different molecular species, to modulate and to extend possible values of the order level of the membrane (Fig. 1).

Beside free sterols, SGs and ASGs are ubiquitously present in vascular plants, where the composition of sterols in SG usually reflects the free sterol composition (33). Interestingly, the proportions of SG and ASG in PM differ greatly depending on the plant species and the growth conditions, varying from 8% SG plus ASG in *Arabidopsis thaliana* leaves to 6% SG and 27% ASG in spring oat (*Avena sativa*) leaf (102, 103). The similar ability of conjugated and free forms of phytosterols alone to order membrane evidenced in this study (Fig. 3) is in agreement with the similar efficiency of steryl glycosides, acylated steryl glycosides, and free sterol mixture isolated from soybean to eliminate the thermal phase transition of dipalmitoyl lecithin (104).

However, the ordering ability of free and conjugated forms is strongly enhanced when these different forms of phytosterols are added in combination (Fig. 3). These data demonstrate an impact of ASG/SG amount on membrane physical properties and suggest that the changes in the ratio of conjugated to free forms of sterol could be a major key to modulate the phase behavior of PM, as observed, for example, during dehydration (105). In agreement with such a model, compensatory changes in free sterol *versus* SG plus ASG suggest an interconversion of the lipids during cold acclimation in rye seedlings (106) or in *A. thaliana* (107).

Plant Lipid Diversity Determines Spatial Organization of Membrane Order Level—Lateral segregation of lipids has been proposed as one of the possible actors in the modulation of membrane physical properties, leading to L_o and L_d phase separation (6, 7). The DOPC (T_m = −20 °C)/DPPC (T_m = 41 °C) lipid mixture, which has been widely used in the literature to characterize the physical properties of the membrane model system (11, 14, 83, 108, 109), exhibits, at temperatures below 45 °C, an L_o and L_d phase coexistence (83). Performing our experiments at 22 °C and minimizing temperature fluctuations, we actually favored a long time equilibrium formation of L_o and L_d phase separation, allowing us to focus our study on the structuring effect of plant lipid on L_o and L_d phase partitioning. Using multispectral confocal microscopy on giant model membranes labeled with di-4-ANEPPDHQ dye, previously shown to be relevant to characterize L_o and L_d phase partitioning (54, 62), we thus identified a sterol-dependent ordered domain formation (Fig. 5). Such ordered phase formation has been previously associated with the appearance of sterol-rich domains (10). We observed here a close correlation between L_o and L_d phases and the sterol-enriched and sterol-deprived areas of the membrane, respectively (Fig. 5), suggesting close correspondence of ordered domains and sterol-rich domains, as proposed in the membrane raft hypothesis (8).

Analysis of spatial organization of the membrane performed in this study demonstrates the differential ability of phytosterols to (i) promote the occurrence of ordered domains within the membrane and (ii) organize them at the membrane surface, both related to their ability to increase the global order level of the bilayer. In agreement with our observation, β-sitosterol, as a relevant example, has been proved to induce the production of numerous small domains, increasing the surface of L_o-L_d transition regions (110). Furthermore, we interestingly propose that combined phytosterols exhibit both an additive/subtractive effect to modulate the global order level of the membrane and a cooperative effect to enhance larger L_o domain formation. The lateral distribution of L_o domains is also strongly affected by the addition of phytosterol-conjugated forms and/or GIPC (Fig. 7*B*). We thus observed that free sterol-sph-

Downloaded from http://www.jbc.org/ at INRA Institut National de la Recherche Agronomique on April 21, 2015

ingolipid and free sterol-SG/ASG combination enhance L_o domain representativeness (Fig. 6*E*) and enlarge ordered domain size (Fig. 6*F*), arguing in favor of the "membrane raft" model (8). Indeed, SG/ASG are enriched in detergent-resistant membranes (32, 111, 112), in good agreement with their ability to promote L_o domain formation. Moreover, gangliosides, which are structural analogs of plant GIPCs in the mammalian model, are commonly used as raft markers (10, 81, 113–115). Our data demonstrate that each plant lipid class could partly account for the complex lateral distribution of ordered domains within the lipid bilayer. One must note that the diversity of molecular lipid species and their specific amount are very different in animal and plant membranes. For example, animal gangliosides are present in very low amounts in animal membrane, less than few percent. This is not at all the case for plant GIPCs, which represent the major sphingolipids (13). In addition, cholesterol is the sole sterol found in mammal membranes compared with the high diversity of sterol mixture in plant PM. Such potency to interact and to subtly and spatially organize the membrane gives sense to the huge diversity of plant membrane lipids.

Different interesting mechanisms could account for the change in vesicle order level induced by lipids. We interestingly observed no correlation between the global order level, as measured using vesicle RGM, and the L_o domain representativeness at the GUV surface, which varies independently when lipids exhibiting ordering ability in LUV are added. For relevant examples, GUVs containing DOPC/DPPC/sitosterol, although exhibiting similar RGM as GUVs containing DOPC/DPPC/TM, display a different L_o domain representativeness (Fig. 6). Moreover, GIPC supplementation, even if it slightly changes the RGM value (Fig. 7), significantly increases the L_o domain amount. These results might support a first mechanism, in which an increase of L_o domain proportion explains the RGM changes observed. A second possibility is that the order has gone up inside L_o domains. In agreement with this hypothesis, GUVs containing either DOPC/DPPC/TM or DOPC/DPPC/stigmasterol show similar L_o domain representativeness, although the first ones exhibit a significantly lower RGM. Likewise, GUVs containing either DOPC/TM or DOPC/DPPC/TM exhibit similar L_o domain amounts (34 and 39%, respectively) even if their respective RGM significantly decreases (from 1.46 to 1.14), showing an increase of order level of L_o domains with the DPPC addition. Finally, when SGs and/or ASGs are added, both the amount and the order level of L_o domains increase, leading to a very high order level of the vesicle membrane.

Altogether, our data interestingly suggested the coexistence of two different mechanisms controlling the local membrane order level, which one accounting for the RGM modification depending on the extra lipid added.

Sphingolipids, Notably GIPCs, Interact with Sterol to Organize L_o Domains—Data acquired in model systems by x-ray diffraction, differential scanning calorimetry, and polarized light microscopy indicated that a SM lamellar gel phase and a liquid crystalline phase containing both SM and PC coexist at room temperature (116). More recently, controversy has arisen because no phase separation for DOPC/bovine brain SM (7:3) occurs at 20 °C (77, 117). Our data show no ability of GIPC, the major plant sphingolipid (51), to order the phospholipid bilayer (Fig. 3) and argue in favor of no extensive phase separation in the binary sphingolipid/phospholipid system.

We, however, showed the ability of GIPCs to increase, in a phytosterol-dependent manner, the global order level of the membrane (Fig. 3), even in the absence of DPPC (Fig. 7), mimicking the SM-cholesterol effect (83). In the mammalian model, lateral partitioning of L_o and L_d phases is thus explained by a preferential interaction of sphingolipids with cholesterol over phospholipids (22), probably due to better shielding from water by the SM headgroup. Their partitioning into L_o phase is favored by the fact that sphingolipids can create a complex network of hydrogen bonds due to the presence of the amide nitrogen, the carbonyl oxygen, and the hydroxyl group positioned in proximity to the water/lipid interface of the bilayer (118). Moreover, the hydrogen bond network between lipids stabilizes a more rigid phase in the bilayer and increases order (119, 120). Plant GIPC long chain base profiles are dominated by t18:0 and t18:1 species in widely varying proportions (t representing trihydroxylated, called phytosphingosine; 0 or 1 for no or one insaturation; for a review, see Ref. 48), and one hydroxyl residue is very often present at position 2 of the fatty acid. We observed a strong ability of GIPCs to induce, in a sterol-dependent manner, L_o domain formation and, in particular, to increase their size (Fig. 7), suggesting that a strong interaction between phytosterols and GIPCs might lead to a well defined phase separation, in agreement with the hydrogen-bond network model. One may hypothesize that the presence of the three hydroxyl groups at the interface between the polar phase and hydrophobic phase of the bilayer may be of importance for phytosphingolipid/phytosterol interactions.

Animal glycosphingolipid with a monosaccharide headgroup is much bulkier than phospholipid ones and occupies a larger volume, as proposed by theoretical calculations of the minimum energy conformation, which results in spontaneous membrane curvature (25). According to these predictions, ganglioside phase separation in model membrane depends on the surface area occupied by the oligosaccharide chain that is usually directly correlated with the number of sugar residues (121–123). The major GIPC polar head is composed of *N*-acetylglucosamine/glucuronic acid/inositol/phosphate, and up to seven sugar moieties can be added, particularly in a tobacco BY-2 cell culture (55), from which GIPCs were isolated in this study. Therefore, the volume occupied by the headgroup of GIPC is far bulkier than phospholipid headgroups, explaining their high propensity for partitioning in L_o domains.

In summary, we demonstrated the ability of free and conjugated forms of phytosterols to modulate the model membrane order. Moreover, we propose that, in the PM of plant cells, phytosterols could be key compounds to mediate the formation of lipid ordered domains, through interactions with other plant lipids, such as GIPCs. Our data allow new insights into how the diversity of plant lipids might drive the PM subcompartmentalization, allowing the dynamic segregation of membrane components, in the framework of the membrane raft hypothesis (124–126). The diversity of plant lipid mixture retrieved in plant cell PM raises the question of the coexistence of lipid domains of various compositions and consequently different

Downloaded from http://www.jbc.org/ at INRA Institut National de la Recherche Agronomique on April 21, 2015

lipid-lipid interactions, which have now to be characterized *in vivo*. Furthermore, the membrane raft hypothesis expands the field of such investigations, suggesting the possible involvement of protein-lipid, membrane-cytoskeleton, and membrane-cell wall interactions that need to be further investigated.

Acknowledgments—We thank Claire Bossard and Paul Gouguet (Laboratoire de Biogenèse Membranaire) for help in the preparation of tobacco BY-2 GIPC. We are grateful to Christophe Der for contributions to the optimization of the microscopy setup and helpful analysis of data.

REFERENCES

1. Grant, C. W., Wu, S. H., and McConnell, H. M. (1974) Lateral phase separations in binary lipid mixtures: correlation between spin label and freeze-fracture electron microscopic studies. *Biochim. Biophys. Acta* **363,** 151–158
2. Lentz, B. R., Barenholz, Y., and Thompson, T. E. (1976) Fluorescence depolarization studies of phase transitions and fluidity in phospholipid bilayers. 2. Two-component phosphatidylcholine liposomes. *Biochemistry* **15,** 4529–4537
3. Phillips, M. C., Kamat, V. B., and Chapman, D. (1970) The interaction of cholesterol with the sterol free lipids of plasma membranes. *Chem. Phys. Lipids* **4,** 409–417
4. Shimshick, E. J., and McConnell, H. M. (1973) Lateral phase separation in phospholipid membranes. *Biochemistry* **12,** 2351–2360
5. Wesołowska, O., Michalak, K., Maniewska, J., and Hendrich, A. B. (2009) Giant unilamellar vesicles: a perfect tool to visualize phase separation and lipid rafts in model systems. *Acta Biochim. Pol.* **56,** 33–39
6. Gebhardt, C., Gruler, H., and Sackmann, E. (1977) On domain structure and local curvature in lipid bilayers and biological membranes. *Z Naturforsch. C* **32,** 581–596
7. Schmidt, C. F., Barenholz, Y., and Thompson, T. E. (1977) A nuclear magnetic resonance study of sphingomyelin in bilayer systems. *Biochemistry* **16,** 2649–2656
8. Lingwood, D., and Simons, K. (2010) Lipid rafts as a membrane-organizing principle. *Science* **327,** 46–50
9. Baumgart, T., Hess, S. T., and Webb, W. W. (2003) Imaging coexisting fluid domains in biomembrane models coupling curvature and line tension. *Nature* **425,** 821–824
10. Dietrich, C., Bagatolli, L. A., Volovyk, Z. N., Thompson, N. L., Levi, M., Jacobson, K., and Gratton, E. (2001) Lipid rafts reconstituted in model membranes. *Biophys. J.* **80,** 1417–1428
11. Scherfeld, D., Kahya, N., and Schwille, P. (2003) Lipid dynamics and domain formation in model membranes composed of ternary mixtures of unsaturated and saturated phosphatidylcholines and cholesterol. *Biophys. J.* **85,** 3758–3768
12. Samsonov, A. V., Mihalyov, I., and Cohen, F. S. (2001) Characterization of cholesterol-sphingomyelin domains and their dynamics in bilayer membranes. *Biophys. J.* **81,** 1486–1500
13. Veatch, S. L., and Keller, S. L. (2002) Organization in lipid membranes containing cholesterol. *Phys. Rev. Lett.* **89,** 268101
14. Veatch, S. L., and Keller, S. L. (2003) Separation of liquid phases in giant vesicles of ternary mixtures of phospholipids and cholesterol. *Biophys. J.* **85,** 3074–3083
15. Quinn, P. J. (2010) A lipid matrix model of membrane raft structure. *Prog. Lipid Res.* **49,** 390–406
16. Quinn, P. J., and Wolf, C. (2009) The liquid-ordered phase in membranes. *Biochim. Biophys. Acta* **1788,** 33–46
17. Mannock, D. A., Lewis, R. N., McMullen, T. P., and McElhaney, R. N. (2010) The effect of variations in phospholipid and sterol structure on the nature of lipid-sterol interactions in lipid bilayer model membranes. *Chem. Phys. Lipids* **163,** 403–448
18. Kim, K., Choi, S. Q., Zell, Z. A., Squires, T. M., and Zasadzinski, J. A. (2013) Effect of cholesterol nanodomains on monolayer morphology and dynamics. *Proc. Natl. Acad. Sci. U.S.A.* **110,** E3054–E3060
19. Frazier, M. L., Wright, J. R., Pokorny, A., and Almeida, P. F. (2007) Investigation of domain formation in sphingomyelin/cholesterol/POPC mixtures by fluorescence resonance energy transfer and Monte Carlo simulations. *Biophys. J.* **92,** 2422–2433
20. Henriksen, J., Rowat, A. C., Brief, E., Hsueh, Y. W., Thewalt, J. L., Zuckermann, M. J., and Ipsen, J. H. (2006) Universal behavior of membranes with sterols. *Biophys. J.* **90,** 1639–1649
21. Jiménez-Rojo, N., García-Arribas, A. B., Sot, J., Alonso, A., and Goñi, F. M. (2014) Lipid bilayers containing sphingomyelins and ceramides of varying *N*-acyl lengths: a glimpse into sphingolipid complexity. *Biochim. Biophys. Acta* **1838,** 456–464
22. Lönnfors, M., Doux, J. P., Killian, J. A., Nyholm, T. K., and Slotte, J. P. (2011) Sterols have higher affinity for sphingomyelin than for phosphatidylcholine bilayers even at equal acyl-chain order. *Biophys. J.* **100,** 2633–2641
23. Pinto, S. N., Fernandes, F., Fedorov, A., Futerman, A. H., Silva, L. C., and Prieto, M. (2013) A combined fluorescence spectroscopy, confocal and 2-photon microscopy approach to re-evaluate the properties of sphingolipid domains. *Biochim. Biophys. Acta* **1828,** 2099–2110
24. Ramstedt, B., and Slotte, J. P. (2006) Sphingolipids and the formation of sterol-enriched ordered membrane domains. *Biochim. Biophys. Acta* **1758,** 1945–1956
25. Sonnino, S., and Prinetti, A. (2010) Lipids and membrane lateral organization. *Front. Physiol.* **1,** 153
26. Furt, F., Lefebvre, B., Cullimore, J., Bessoule, J. J., and Mongrand, S. (2007) Plant lipid rafts: fluctuat nec mergitur. *Plant Signal. Behav.* **2,** 508–511
27. Guo, D. A., Venkatramesh, M., and Nes, W. D. (1995) Developmental regulation of sterol biosynthesis in Zea-Mays. *Lipids* **30,** 203–219
28. Schaller, H. (2004) New aspects of sterol biosynthesis in growth and development of higher plants. *Plant Physiol. Biochem.* **42,** 465–476
29. Grille, S., Zaslawski, A., Thiele, S., Plat, J., and Warnecke, D. (2010) The functions of steryl glycosides come to those who wait: recent advances in plants, fungi, bacteria and animals. *Prog. Lipid Res.* **49,** 262–288
30. Heinz, E. (1996) *Plant Glycolipids: Structure, Isolation and Analysis*, Vol. 3 (Christie, W. W., ed) pp. 211–332, The Oily Press, Dundee, United Kingdom
31. Kovganko, N. V., and Kashkan, Zh. N. (1999) Sterol glycosides and acylglycosides. *Chem. Nat. Compd.* **35,** 479–497
32. Lefebvre, B., Furt, F., Hartmann, M. A., Michaelson, L. V., Carde, J. P., Sargueil-Boiron, F., Rossignol, M., Napier, J. A., Cullimore, J., Bessoule, J. J., and Mongrand, S. (2007) Characterization of lipid rafts from *Medicago truncatula* root plasma membranes: a proteomic study reveals the presence of a raft-associated redox system. *Plant Physiol.* **144,** 402–418
33. Wojciechowski, Z. A. (ed) (1991) *Biochemistry of Phytosterol Conjugates*, American Oil Chemists Society, Urbana, IL
34. Wewer, V., Dombrink, I., vom Dorp, K., and Dörmann, P. (2011) Quantification of sterol lipids in plants by quadrupole time-of-flight mass spectrometry. *J. Lipid Res.* **52,** 1039–1054
35. Schrick, K., Shiva, S., Arpin, J. C., Delimont, N., Isaac, G., Tamura, P., and Welti, R. (2012) Steryl glucoside and acyl steryl glucoside analysis of *Arabidopsis* seeds by electrospray ionization tandem mass spectrometry. *Lipids* **47,** 185–193
36. Webb, M. S., Irving, T. C., and Steponkus, P. L. (1995) Effects of plant sterols on the hydration and phase behavior of DOPE/DOPC mixtures. *Biochim. Biophys. Acta* **1239,** 226–238
37. Brown, D. A., and Rose, J. K. (1992) Sorting of GPI-anchored proteins to glycolipid-enriched membrane subdomains during transport to the apical cell surface. *Cell* **68,** 533–544
38. Markham, J. E., Li, J., Cahoon, E. B., and Jaworski, J. G. (2006) Separation and identification of major plant sphingolipid classes from leaves. *J. Biol. Chem.* **281,** 22684–22694
39. Cacas, J. L., Furt, F., Le Guédard, M., Schmitter, J. M., Buré, C., Gerbeau-Pissot, P., Moreau, P., Bessoule, J. J., Simon-Plas, F., and Mongrand, S. (2012) Lipids of plant membrane rafts. *Prog. Lipid Res.* **51,** 272–299
40. Carter, H. E., Gigg, R. H., Law, J. H., Nakayama, T., and Weber, E. (1958) Biochemistry of the sphingolipides. XI. Structure of phytoglycolipide. *J. Biol. Chem.* **233,** 1309–1314

Downloaded from http://www.jbc.org/ at INRA Institut National de la Recherche Agronomique on April 21, 2015

41. Carter, H. E., and Koob, J. L. (1969) Sphingolipids in bean leaves (*Phaseolus vulgaris*). *J. Lipid Res.* **10,** 363–369
42. Hsieh, T. C., Kaul, K., Laine, R. A., and Lester, R. L. (1978) Structure of a major glycophosphoceramide from tobacco leaves, PSL-I: 2-deoxy-2-acetamido-D-glucopyranosyl(α1→4)-D-glucuronopyranosyl-(α1→2)myoinositol-1-*O*-phosphoceramide. *Biochemistry* **17,** 3575–3581
43. Hsieh, T. C., Lester, R. L., and Laine, R. A. (1981) Glycophosphoceramides from plants: purification and characterization of a novel tetrasaccharide derived from tobacco leaf glycolipids. *J. Biol. Chem.* **256,** 7747–7755
44. Kaul, K., and Lester, R. L. (1975) Characterization of inositol-containing phosphosphingolipids from tobacco leaves: isolation and identification of two novel, major lipids: *N*-acetylglucosamidoglucuronidoinositol phosphorylceramide and glucosamidoglucuronidoinositol phosphorylceramide. *Plant Physiol.* **55,** 120–129
45. Spassieva, S. D., Markham, J. E., and Hille, J. (2002) The plant disease resistance gene Asc-1 prevents disruption of sphingolipid metabolism during AAL-toxin-induced programmed cell death. *Plant J.* **32,** 561–572
46. Sperling, P., Franke, S., Lüthje, S., and Heinz, E. (2005) Are glucocerebrosides the predominant sphingolipids in plant plasma membranes? *Plant Physiol. Biochem.* **43,** 1031–1038
47. Hannun, Y. A., and Obeid, L. M. (2008) Principles of bioactive lipid signalling: lessons from sphingolipids. *Nat. Rev. Mol. Cell Biol.* **9,** 139–150
48. Pata, M. O., Hannun, Y. A., and Ng, C. K. (2010) Plant sphingolipids: decoding the enigma of the Sphinx. *New Phytol.* **185,** 611–630
49. Wang, W., Yang, X., Tangchaiburana, S., Ndeh, R., Markham, J. E., Tsegaye, Y., Dunn, T. M., Wang, G. L., Bellizzi, M., Parsons, J. F., Morrissey, D., Bravo, J. E., Lynch, D. V., and Xiao, S. (2008) An inositolphosphorylceramide synthase is involved in regulation of plant programmed cell death associated with defense in *Arabidopsis*. *Plant Cell* **20,** 3163–3179
50. Cacas, J. L., Buré, C., Furt, F., Maalouf, J. P., Badoc, A., Cluzet, S., Schmitter, J. M., Antajan, E., and Mongrand, S. (2013) Biochemical survey of the polar head of plant glycosylinositolphosphoceramides unravels broad diversity. *Phytochemistry* **96,** 191–200
51. Buré, C., Cacas, J. L., Mongrand, S., and Schmitter, J. M. (2014) Characterization of glycosyl inositol phosphoryl ceramides from plants and fungi by mass spectrometry. *Anal. Bioanal. Chem.* **406,** 995–1010
52. Obaid, A. L., Loew, L. M., Wuskell, J. P., and Salzberg, B. M. (2004) Novel naphthylstyryl-pyridium potentiometric dyes offer advantages for neural network analysis. *J. Neurosci. Methods* **134,** 179–190
53. Jin, L., Millard, A. C., Wuskell, J. P., Clark, H. A., and Loew, L. M. (2005) Cholesterol-enriched lipid domains can be visualized by di-4-ANEPPDHQ with linear and nonlinear optics. *Biophys. J.* **89,** L04–L06
54. Jin, L., Millard, A. C., Wuskell, J. P., Dong, X., Wu, D., Clark, H. A., and Loew, L. M. (2006) Characterization and application of a new optical probe for membrane lipid domains. *Biophys. J.* **90,** 2563–2575
55. Buré, C., Cacas, J. L., Wang, F., Gaudin, K., Domergue, F., Mongrand, S., and Schmitter, J. M. (2011) Fast screening of highly glycosylated plant sphingolipids by tandem mass spectrometry. *Rapid Commun. Mass Spectrom.* **25,** 3131–3145
56. Angelova, M. I., Soleau, S., Meleard, P., Faucon, J. F., and Bothorel, P. (1992) Preparation of giant vesicles by external AC electric fields. *Prog. Colloid Polym. Sci.* **89,** 127–131
57. Dimitrov, D. S., and Angelova, M. I. (1988) Lipid swelling and liposome electroformation mediated by electric fields. *Bioelectrochem. Bioenerg.* **19,** 323–333
58. Menger, F. M., and Angelova, M. I. (1998) Giant vesicles: imitating the cytological processes of cell membranes. *Acc. Chem. Res.* **31,** 789–797
59. MacDonald, R. C., MacDonald, R. I., Menco, B. P., Takeshita, K., Subbarao, N. K., and Hu, L. R. (1991) Small-volume extrusion apparatus for preparation of large, unilamellar vesicles. *Biochim. Biophys. Acta* **1061,** 297–303
60. Subbarao, N. K., MacDonald, R. I., Takeshita, K., and MacDonald, R. C. (1991) Characteristics of spectrin-induced leakage of extruded, phosphatidylserine vesicles. *Biochim. Biophys. Acta* **1063,** 147–154
61. Millard, A. C., Jin, L., Wei, M. D., Wuskell, J. P., Lewis, A., and Loew, L. M. (2004) Sensitivity of second harmonic generation from styryl dyes to transmembrane potential. *Biophys. J.* **86,** 1169–1176
62. Owen, D. M., and Gaus, K. (2010) Optimized time-gated generalized polarization imaging of Laurdan and di-4-ANEPPDHQ for membrane order image contrast enhancement. *Microsc. Res. Tech.* **73,** 618–622
63. Owen, D. M., Rentero, C., Magenau, A., Abu-Siniyeh, A., and Gaus, K. (2012) Quantitative imaging of membrane lipid order in cells and organisms. *Nat. Protoc.* **7,** 24–35
64. Bonneau, L., Gerbeau-Pissot, P., Thomas, D., Der, C., Lherminier, J., Bourque, S., Roche, Y., and Simon-Plas, F. (2010) Plasma membrane sterol complexation, generated by filipin, triggers signaling responses in tobacco cells. *Biochim. Biophys. Acta* **1798,** 2150–2159
65. Dinic, J., Ashrafzadeh, P., and Parmryd, I. (2013) Actin filaments attachment at the plasma membrane in live cells cause the formation of ordered lipid domains. *Biochim. Biophys. Acta* **1828,** 1102–1111
66. Dinic, J., Biverståhl, H., Mäler, L., and Parmryd, I. (2011) Laurdan and di-4-ANEPPDHQ do not respond to membrane-inserted peptides and are good probes for lipid packing. *Biochim. Biophys. Acta* **1808,** 298–306
67. Gerbeau-Pissot, P., Der, C., Thomas, D., Anca, I. A., Grosjean, K., Roche, Y., Perrier-Cornet, J. M., Mongrand, S., and Simon-Plas, F. (2014) Modification of plasma membrane organization in tobacco cells elicited by cryptogein. *Plant Physiol.* **164,** 273–286
68. Liu, P., Li, R. L., Zhang, L., Wang, Q. L., Niehaus, K., Baluska, F., Samaj, J., and Lin, J. X. (2009) Lipid microdomain polarization is required for NADPH oxidase-dependent ROS signaling in *Picea meyeri* pollen tube tip growth. *Plant J.* **60,** 303–313
69. Roche, Y., Gerbeau-Pissot, P., Buhot, B., Thomas, D., Bonneau, L., Gresti, J., Mongrand, S., Perrier-Cornet, J. M., and Simon-Plas, F. (2008) Depletion of phytosterols from the plant plasma membrane provides evidence for disruption of lipid rafts. *FASEB J.* **22,** 3980–3991
70. Roche, Y., Klymchenko, A. S., Gerbeau-Pissot, P., Gervais, P., Mély, Y., Simon-Plas, F., and Perrier-Cornet, J. M. (2010) Behavior of plant plasma membranes under hydrostatic pressure as monitored by fluorescent environment-sensitive probes. *Biochim. Biophys. Acta* **1798,** 1601–1607
71. Uline, M. J., and Szleifer, I. (2013) Mode specific elastic constants for the gel, liquid-ordered, and liquid-disordered phases of DPPC/DOPC/cholesterol model lipid bilayers. *Faraday Discuss.* **161,** 177–191; discussion 273–303
72. de Joannis, J., Coppock, P. S., Yin, F., Mori, M., Zamorano, A., and Kindt, J. T. (2011) Atomistic simulation of cholesterol effects on miscibility of saturated and unsaturated phospholipids: implications for liquid-ordered/liquid-disordered phase coexistence. *J. Am. Chem. Soc.* **133,** 3625–3634
73. Almeida, P. F. (2011) A simple thermodynamic model of the liquid-ordered state and the interactions between phospholipids and cholesterol. *Biophys. J.* **100,** 420–429
74. Marsh, D. (2010) Liquid-ordered phases induced by cholesterol: a compendium of binary phase diagrams. *Biochim. Biophys. Acta* **1798,** 688–699
75. Clarke, J. A., Heron, A. J., Seddon, J. M., and Law, R. V. (2006) The diversity of the liquid ordered (Lo) phase of phosphatidylcholine/cholesterol membranes: a variable temperature multinuclear solid-state NMR and x-ray diffraction study. *Biophys. J.* **90,** 2383–2393
76. Ouimet, J., and Lafleur, M. (2004) Hydrophobic match between cholesterol and saturated fatty acid is required for the formation of lamellar liquid ordered phases. *Langmuir* **20,** 7474–7481
77. Ahmed, S. N., Brown, D. A., and London, E. (1997) On the origin of sphingolipid/cholesterol-rich detergent-insoluble cell membranes: physiological concentrations of cholesterol and sphingolipid induce formation of a detergent-insoluble, liquid-ordered lipid phase in model membranes. *Biochemistry* **36,** 10944–10953
78. Reinl, H., Brumm, T., and Bayerl, T. M. (1992) Changes of the physical properties of the liquid-ordered phase with temperature in binary mixtures of DPPC with cholesterol: a H-NMR, FT-IR, DSC, and neutron scattering study. *Biophys. J.* **61,** 1025–1035
79. Fujino, Y., Ohnishi, M., and Ito, S. (1985) Molecular species of ceramide and mono-, di-, tri-, and tetraglycosylceramide in bran and endosperm of rice grains. *Agric. Biol. Chem.* **49,** 2753–2762
80. Islam, M. N., Chambers, J. P., and Ng, C. K.-Y. (2012) Lipid profiling of

Downloaded from http://www.jbc.org/ at INRA Institut National de la Recherche Agronomique on April 21, 2015

the model temperate grass, *Brachypodium distachyon*. *Metabolomics* 10.1007/s11306-011-0352-x
81. Kahya, N., Scherfeld, D., Bacia, K., Poolman, B., and Schwille, P. (2003) Probing lipid mobility of raft-exhibiting model membranes by fluorescence correlation spectroscopy. *J. Biol. Chem.* **278,** 28109–28115
82. Ariola, F. S., Li, Z., Cornejo, C., Bittman, R., and Heikal, A. A. (2009) Membrane fluidity and lipid order in ternary giant unilamellar vesicles using a new bodipy-cholesterol derivative. *Biophys. J.* **96,** 2696–2708
83. Aguilar, L. F., Pino, J. A., Soto-Arriaza, M. A., Cuevas, F. J., Sánchez, S., and Sotomayor, C. P. (2012) Differential dynamic and structural behavior of lipid-cholesterol domains in model membranes. *PLoS One* **7,** e40254
84. Ranadive, G. N., and Lala, A. K. (1987) Sterol-phospholipid interaction in model membranes: role of C5-C6 double bond in cholesterol. *Biochemistry* **26,** 2426–2431
85. Stillwell, W., and Wassall, S. R. (1990) Interactions of retinoids with phospholipid membranes: optical spectroscopy. *Methods Enzymol.* **189,** 373–382
86. Schuler, I., Milon, A., Nakatani, Y., Ourisson, G., Albrecht, A. M., Benveniste, P., and Hartman, M. A. (1991) Differential effects of plant sterols on water permeability and on acyl chain ordering of soybean phosphatidylcholine bilayers. *Proc. Natl. Acad. Sci. U.S.A.* **88,** 6926–6930
87. Demel, R. A., Bruckdorfer, K. R., and van Deenen, L. L. (1972) The effect of sterol structure on the permeability of lipomes to glucose, glycerol and Rb +. *Biochim. Biophys. Acta* **255,** 321–330
88. Demel, R. A., Bruckdorfer, K. R., and van Deenen, L. L. (1972) Structural requirements of sterols for the interaction with lecithin at the air water interface. *Biochim. Biophys. Acta* **255,** 311–320
89. Verkleij, A. J., de Kruijff, B., Gerritsen, W. F., Demel, R. A., van Deenen, L. L., and Ververgaert, P. H. (1973) Freeze-etch electron microscopy of erythrocytes, *Acholeplasma laidlawii* cells and liposomal membranes after the action of filipin and amphotericin B. *Biochim. Biophys. Acta* **291,** 577–581
90. Halling, K. K., and Slotte, J. P. (2004) Membrane properties of plant sterols in phospholipid bilayers as determined by differential scanning calorimetry, resonance energy transfer and detergent-induced solubilization. *Biochim. Biophys. Acta* **1664,** 161–171
91. Bruckdorfer, K. R., Graham, J. M., and Green, C. (1968) The incorporation of steroid molecules into lecithin sols, β-lipoproteins and cellular membranes. *Eur. J. Biochem.* **4,** 512–518
92. Edwards, P. A., and Green, C. (1972) Incorporation of plant sterols into membranes and its relation to sterol absorption. *FEBS Lett.* **20,** 97–99
93. Schuler, I., Duportail, G., Glasser, N., Benveniste, P., and Hartmann, M. A. (1990) Soybean phosphatidylcholine vesicles containing plant sterols: a fluorescence anisotropy study. *Biochim. Biophys. Acta* **1028,** 82–88
94. Rujanavech, C., Henderson, P. A., and Silbert, D. F. (1986) Influence of sterol structure on phospholipid phase behavior as detected by parinaric acid fluorescence spectroscopy. *J. Biol. Chem.* **261,** 7204–7214
95. Hartmann, M. A. (1998) Plant sterols and the membrane environment. *Trends Plant Sci.* 10.1016/S1360-1385(98)01233-3
96. Quartacci, M. F., Glisić, O., Stevanović, B., and Navari-Izzo, F. (2002) Plasma membrane lipids in the resurrection plant *Ramonda serbica* following dehydration and rehydration. *J. Exp. Bot.* **53,** 2159–2166
97. López-Pérez, L., Martínez-Ballesta Mdel, C., Maurel, C., and Carvajal, M. (2009) Changes in plasma membrane lipids, aquaporins and proton pump of broccoli roots, as an adaptation mechanism to salinity. *Phytochemistry* **70,** 492–500
98. Arnqvist, L., Persson, M., Jonsson, L., Dutta, P. C., and Sitbon, F. (2008) Overexpression of CYP710A1 and CYP710A4 in transgenic *Arabidopsis* plants increases the level of stigmasterol at the expense of sitosterol. *Planta* **227,** 309–317
99. Wang, K., Senthil-Kumar, M., Ryu, C. M., Kang, L., and Mysore, K. S. (2012) Phytosterols play a key role in plant innate immunity against bacterial pathogens by regulating nutrient efflux into the apoplast. *Plant Physiol.* **158,** 1789–1802
100. Benz, R., and Cros, D. (1978) Influence of sterols on ion transport through lipid bilayer membranes. *Biochim. Biophys. Acta* **506,** 265–280
101. Berglund, A. H., Quartacci, M. F., Calucci, L., Navari-Izzo, F., Pinzino, C., and Liljenberg, C. (2002) Alterations of wheat root plasma membrane lipid composition induced by copper stress result in changed physicochemical properties of plasma membrane lipid vesicles. *Biochim. Biophys. Acta* **1564,** 466–472
102. Uemura, M., Joseph, R. A., and Steponkus, P. L. (1995) Cold acclimation of *Arabidopsis thaliana* (effect on plasma membrane lipid composition and freeze-induced lesions). *Plant Physiol.* **109,** 15–30
103. Uemura, M., and Steponkus, P. L. (1994) A contrast of the plasma membrane lipid composition of oat and rye leaves in relation to freezing tolerance. *Plant Physiol.* **104,** 479–496
104. Mudd, J. B., and McManus, T. T. (1980) Effect of steryl glycosides on the phase transition of dipalmitoyl lecithin. *Plant Physiol.* **65,** 78–80
105. Palta, J. P., Whitaker, B. D., and Weiss, L. S. (1993) Plasma membrane lipids associated with genetic variability in freezing tolerance and cold acclimation of solanum species. *Plant Physiol.* **103,** 793–803
106. Lynch, D. V., and Steponkus, P. L. (1987) Plasma membrane lipid alterations associated with cold acclimation of winter rye seedlings (*Secale cereale* L. cv. Puma). *Plant Physiol.* **83,** 761–767
107. Minami, A., Furuto, A., and Uemura, M. (2010) Dynamic compositional changes of detergent-resistant plasma membrane microdomains during plant cold acclimation. *Plant Signal. Behav.* **5,** 1115–1118
108. Parasassi, T., Gratton, E., Yu, W. M., Wilson, P., and Levi, M. (1997) Two-photon fluorescence microscopy of laurdan generalized polarization domains in model and natural membranes. *Biophys. J.* **72,** 2413–2429
109. Stevens, M. M., Honerkamp-Smith, A. R., and Keller, S. L. (2010) Solubility limits of cholesterol, lanosterol, ergosterol, stigmasterol, and β-sitosterol in electroformed lipid vesicles. *Soft Matter* **6,** 5882–5890
110. Beck, J. G., Mathieu, D., Loudet, C., Buchoux, S., and Dufourc, E. J. (2007) Plant sterols in "rafts": a better way to regulate membrane thermal shocks. *FASEB J.* **21,** 1714–1723
111. Minami, A., Fujiwara, M., Furuto, A., Fukao, Y., Yamashita, T., Kamo, M., Kawamura, Y., and Uemura, M. (2009) Alterations in detergent-resistant plasma membrane microdomains in *Arabidopsis thaliana* during cold acclimation. *Plant Cell Physiol.* **50,** 341–359
112. Mongrand, S., Morel, J., Laroche, J., Claverol, S., Carde, J. P., Hartmann, M. A., Bonneu, M., Simon-Plas, F., Lessire, R., and Bessoule, J. J. (2004) Lipid rafts in higher plant cells: purification and characterization of Triton X-100-insoluble microdomains from tobacco plasma membrane. *J. Biol. Chem.* **279,** 36277–36286
113. Janich, P., and Corbeil, D. (2007) GM1 and GM3 gangliosides highlight distinct lipid microdomains within the apical domain of epithelial cells. *FEBS Lett.* **581,** 1783–1787
114. Lingwood, D., Ries, J., Schwille, P., and Simons, K. (2008) Plasma membranes are poised for activation of raft phase coalescence at physiological temperature. *Proc. Natl. Acad. Sci. U.S.A.* **105,** 10005–10010
115. Sezgin, E., Levental, I., Grzybek, M., Schwarzmann, G., Mueller, V., Honigmann, A., Belov, V. N., Eggeling, C., Coskun, U., Simons, K., and Schwille, P. (2012) Partitioning, diffusion, and ligand binding of raft lipid analogs in model and cellular plasma membranes. *Biochim. Biophys. Acta* **1818,** 1777–1784
116. Barenholz, Y., and Thompson, T. E. (1980) Sphingomyelins in bilayers and biological membranes. *Biochim. Biophys. Acta* **604,** 129–158
117. Gandhavadi, M., Allende, D., Vidal, A., Simon, S. A., and McIntosh, T. J. (2002) Structure, composition, and peptide binding properties of detergent soluble bilayers and detergent resistant rafts. *Biophys. J.* **82,** 1469–1482
118. Pascher, I. (1976) Molecular arrangements in sphingolipids: conformation and hydrogen bonding of ceramide and their implication on membrane stability and permeability. *Biochim. Biophys. Acta* **455,** 433–451
119. Mombelli, E., Morris, R., Taylor, W., and Fraternali, F. (2003) Hydrogen-bonding propensities of sphingomyelin in solution and in a bilayer assembly: a molecular dynamics study. *Biophys. J.* **84,** 1507–1517
120. Pandit, S. A., Vasudevan, S., Chiu, S. W., Mashl, R. J., Jakobsson, E., and Scott, H. L. (2004) Sphingomyelin-cholesterol domains in phospholipid membranes: atomistic simulation. *Biophys. J.* **87,** 1092–1100
121. Masserini, M., and Freire, E. (1986) Thermotropic characterization of

Downloaded from http://www.jbc.org/ at INRA Institut National de la Recherche Agronomique on April 21, 2015

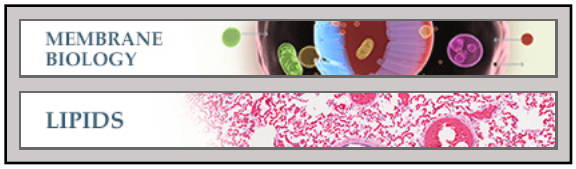
phosphatidylcholine vesicles containing ganglioside GM1 with homogeneous ceramide chain length. *Biochemistry* **25,** 1043–1049
122. Masserini, M., Palestini, P., and Freire, E. (1989) Influence of glycolipid oligosaccharide and long-chain base composition on the thermotropic properties of dipalmitoylphosphatidylcholine large unilamellar vesicles containing gangliosides. *Biochemistry* **28,** 5029–5034
123. Masserini, M., Palestini, P., Venerando, B., Fiorilli, A., Acquotti, D., and Tettamanti, G. (1988) Interactions of proteins with ganglioside-enriched microdomains on the membrane: the lateral phase separation of molecular species of GD1a ganglioside, having homogeneous long-chain base composition, is recognized by *Vibrio cholerae* sialidase. *Biochemistry* **27,** 7973–7978
124. Bagatolli, L. A., and Mouritsen, O. G. (2013) Is the fluid mosaic (and the accompanying raft hypothesis) a suitable model to describe fundamental features of biological membranes? What may be missing? *Front. Plant Sci.* **4,** 457
125. Kusumi, A., and Suzuki, K. (2005) Toward understanding the dynamics of membrane-raft-based molecular interactions. *Biochim. Biophys. Acta* **1746,** 234–251
126. Kusumi, A., Suzuki, K. G., Kasai, R. S., Ritchie, K., and Fujiwara, T. K. (2011) Hierarchical mesoscale domain organization of the plasma membrane. *Trends Biochem. Sci.* **36,** 604–615

Downloaded from http://www.jbc.org/ at INRA Institut National de la Recherche Agronomique on April 21, 2015



Membrane Biology:

Differential Effect of Plant Lipids on Membrane Organization: SPECIFICITIES OF PHYTOSPHINGOLIPIDS AND PHYTOSTEROLS



Kevin Grosjean, Sébastien Mongrand, Laurent Beney, Françoise Simon-Plas and Patricia Gerbeau-Pissot

J. Biol. Chem. 2015, 290:5810-5825.
doi: 10.1074/jbc.M114.598805 originally published online January 9, 2015

Access the most updated version of this article at doi: 10.1074/jbc.M114.598805

Find articles, minireviews, Reflections and Classics on similar topics on the JBC Affinity Sites.

Alerts:
- When this article is cited
- When a correction for this article is posted

Click here to choose from all of JBC's e-mail alerts

This article cites 125 references, 26 of which can be accessed free at
http://www.jbc.org/content/290/9/5810.full.html#ref-list-1

Downloaded from http://www.jbc.org/ at INRA Institut National de la Recherche Agronomique on April 21, 2015